

LRH: O.D. JORDAN ET AL.

RRH: STRATIGRAPHIC ARCHITECTURE OF THE CRETACEOUS CLIFFHOUSE SANDSTONE, NEW MEXICO, U.S.A.

Research Article

DOI: <http://dx.doi.org/10.2110/jsr.2016.83>

PRESERVED STRATIGRAPHIC ARCHITECTURE AND EVOLUTION OF A NET-TRANSGRESSIVE MIXED WAVE- AND TIDE-INFLUENCED COASTAL SYSTEM: CLIFF HOUSE SANDSTONE, NORTHWESTERN NEW MEXICO, U.S.A.

OLIVER D. JORDAN,* SANJEEV GUPTA, GARY J. HAMPSON, AND HOWARD D. JOHNSON

Department of Earth Science and Engineering, South Kensington Campus, Imperial College, London SW7 2AZ, U.K.

e-mail: olijo@ Statoil.com

*Present Address: Statoil (U.K.), London W2 6BD, U.K.

ABSTRACT: The Cretaceous Cliff House Sandstone comprises a thick (400 m) net-transgressive succession representing a mixed wave- and tide-influenced shallow-marine system that migrated episodically landwards. This study examines the youngest part (middle Campanian) of the Cliff House Sandstone, exposed in Chaco Cultural Natural Historical Park, northwest New Mexico, U.S.A. Detailed mapping of facies architecture between a three-dimensional network of measured sections has allowed the character, geometry, and distribution of key stratigraphic surfaces and stratal units to be reconstructed. Upward-shallowing facies successions (parasequences) are separated by laterally extensive transgressive erosion (ravinement) surfaces cut by both wave and tide processes. Preservation of facies tracts in each parasequence is controlled by the depth of erosion and migration trajectory of the overlying ravinement surfaces. In most parasequences, there is no preservation of the proximal wave-dominated facies tracts (foreshore, upper-shoreface), resulting in thin (4–7 m) top-truncated packages. Four distinct shallow marine tongues (parasequence sets) have been identified, consisting of ten parasequences with a total stratigraphic thickness of ~ 100 m. Each tongue records an episode of complex shoreline migration history (multiple regressive–transgressive phases) in an overall net-transgressive system.

The ravinement surfaces provide a stratigraphic framework in which to understand partitioning of tide- and wave-dominated deposits in a net-transgressive system, and a model is presented to account for the sediment distribution and stratigraphic architecture observed in each parasequence. Despite a complex internal architecture, parasequences exhibit a predictable pattern which can be related to the regressive and transgressive phases of deposition. Preservation of wave-dominated facies tracts is associated with shoreline regression, while tide-dominated facies tracts are interpreted to record sediment accumulation during shoreline transgression that also resulted in significant erosion of the underlying regressive deposits. The interplay between erosion, sediment bypass, and deposition during regression and transgression is shown to ultimately control the preservation and stratigraphic architecture of the larger-scale net-transgressive coastal system. While the Cliff House Sandstone exhibits a facies composition and quantitative stacking patterns (shoreline trajectory) similar to other studied examples, differences in the dip-extent of the wave-dominated sandstone tongue has resulted in a more

disconnected architecture between the high-frequency cycles. Understanding the variety of stratal geometries that ravinement surfaces can generate is therefore crucial to predicting the spatial distribution and facies architecture in transgressive systems.

INTRODUCTION

Transgressive shallow-marine deposits are commonly regarded as being relatively thin, with complex internal geometries, and containing abundant fine-grained intervals (Belknap and Kraft 1981; Demarest and Kraft 1987). These characteristics arise from incomplete preservation and pronounced reworking of shoreline systems during their overall retreat (e.g., Curray 1964), however, thick net-transgressive shallow-marine successions containing abundant stacked sandbodies have been documented (Olsen et al. 1999; Allen and Johnson 2011). Conceptual models indicate that preservation of net-transgressive shallow-marine strata requires overall retreat of the shoreline punctuated by periods of limited shoreline regression (e.g., Swift 1968; Swift et al. 1991; Cattaneo and Steel 2000). Field studies have provided supporting evidence in the form of detailed facies relationships and stratigraphic architectures that match the model predictions (Sixsmith et al. 2008; Allen and Johnson 2011) though the number of field cases documented are significantly fewer than those for regressive systems. Regressive stratigraphic architectures in modern and ancient shallow-marine systems (e.g., Rodriguez et al. 2001; Hampson and Howell 2005; Tamura et al. 2008) have been well documented, but relatively few have attempted to document the transgressive deposits in similar detail, outside of incised-valley fills. As a consequence, there are presently few published models for the internal architecture of net-transgressive shallow-marine systems of the type that exist for their regressive counterparts.

Our understanding of net-transgressive sandstones is limited because modern sand-rich systems are difficult to study directly, and because studies of modern systems do not address the issue of long-term preservation in the stratigraphic record. In the subsurface, key geometrical stratal relationships are too small in scale or are not marked by sufficiently large impedance contrasts to be imaged in seismic data of net-transgressive sandstones. The significance of the numerous vertically stacked sandbodies that occur in thick, net-transgressive systems, and associated three-dimensional stratigraphic architectures are thus poorly constrained. In order to understand these aspects, it is necessary to reconstruct the history of shoreline migration, and the concomitant migration of linked erosional and depositional facies tracts.

Herein we document the detailed stratigraphic architecture of a thick, net-transgressive shallow-marine sandstone that is exceptionally well exposed: the Cliff House Sandstone in Chaco Cultural Natural Historical Park, northwest New Mexico, U.S.A. The Cliff House Sandstone crops out around the perimeter of, and is extensively penetrated by, wells in the center of the San Juan Basin in northwestern New Mexico and southwestern Colorado, where it comprises a mixed wave- and tide-dominated succession of stacked seaward- to landward-stepping units that record an overall transgression (Palmer and Scott 1984; Molenaar 1983; Donselaar 1989; Olsen et al. 1999). Our mapping of facies architecture in a series of adjacent, depositional-dip-oriented canyons in Chaco Cultural Natural Historical Park has enabled quantitative three-dimensional reconstruction of key stratigraphic surfaces and sandbody distributions from near the local up-dip to down-dip pinch-outs of the transgressive sandstone complex. The aims of

this paper are: (i) to document styles of interaction between the coeval facies tracts in the Cliff House Sandstone depositional system(s); (ii) to identify the degree of preservation of tide- and wave-dominated facies beneath erosional surfaces associated with transgression; (iii) to reconstruct the history of shoreline migration, and the distribution of related erosional surfaces; and (iv) to generate a conceptual model to account for sediment partitioning and preservation in a thick, net-transgressive succession.

GEOLOGIC SETTING

The Cliff House Sandstone comprises the transgressive portion of a large regressive–transgressive wedge developed during the Campanian along part of the western margin of the Western Interior Seaway, which extended across the North American continent (Fig. 1A) (Molenaar 1983; Krystinik and DeJarnett 1995). Both the Cliff House Sandstone and the underlying, regressive Point Lookout Sandstone belong to the Mesaverde Group (Fig. 1B). The Cliff House Sandstone is diachronous, and records an overall shoreline retreat of over 170 km from northeast to southwest during a period of c. 4 Myr (Fig. 1B). In any particular location, the Cliff House Sandstone represents only a fraction of this shoreline displacement and duration.

The Western Interior Seaway developed during a period of high global sea level (Miller et al. 2005) and pronounced tectonic subsidence of the interior of the North American continent, driven by thrust-induced loading from the Sevier orogenic belt and more widespread dynamic subsidence above the subducting Farallon Plate to the west (Fig. 1A) (Pang and Nummedal 1995; Liu and Nummedal 2004.). Campanian strata along the western margin of the seaway record the interplay between tectonic and climatic controls on sediment delivery from the Mogollon Highlands and Sevier Orogenic Belt hinterland, tectonic subsidence in the basin, and eustatic sea-level variations (Krystinik and DeJarnett 1995). The Cliff House Sandstone crops out along the flanks of the San Juan Basin, which developed during the early Tertiary Laramide Orogeny, in northeastern New Mexico and southwestern Colorado.

DATA AND METHODS

The study area lies within Chaco Culture National Historical Park, where the upper part of the Cliff House Sandstone crops out (Scott et al. 1984). Within the study area, data have been collected from a series of large, dissected mesas which surround a central canyon, Chaco Canyon. Fifty measured sections detail vertical facies relationships in the upper 100 m of the Cliff House Sandstone (Fig. 2). The lateral extent and geometry of the key stratigraphic surfaces have been mapped between measured sections and across the study area, and these surfaces bound packages of genetically related strata. These data have been used to construct three dip-oriented (southwest to northeast) correlation panels ranging between 5 km and 10 km in length, which encompass the up-dip and down-dip pinchouts of several major sandbodies. In addition, a correlation panel oriented along depositional strike (northwest to southeast) have been constructed along the northern and southern faces of Chaco Canyon. The data density and distribution therefore provides a high-resolution, three-dimensional dataset covering approximately 10 km × 10 km.

FACIES AND FACIES ASSOCIATIONS

The Cliff House Sandstone comprises twelve facies types which occur within three distinct facies associations (Figs 3, 4, 5), reflecting the main sedimentary environments at the time of deposition (Table 1). The tidal channel-fill (T1) and proximal lower-shoreface

(W3) facies account for most of the preserved succession (90% of shallow-marine deposits) exposed in the study area. It is likely that the uppermost, fine-grained strata of the studied succession, consisting of distal lower-shoreface (W4) and offshore shales (W5), have been removed by Quaternary erosion.

Continental Facies Association

The continental facies association is mainly exposed in the lower and more proximal part of the Cliff House Sandstone in the southwestern part of the study area. They are overlain by and pass down-dip into tide-dominated and wave-dominated facies associations, and are often intercalated with the former.

Undifferentiated Coastal-Plain and Lagoonal Facies (C1)

Description.—This facies is composed of interbedded fine- to medium-grained sheet sandstones (0.1–0.5 m thick) with carbonaceous mudstones and discontinuous coal seams (Fig. 3A). The sandstones consist of moderately sorted, sub-rounded grains and exhibit ripple cross-lamination. In addition, vertical to sub-vertical, downward-tapering, semi-cylindrical tubes of 0.05–0.1 m in length are locally observed. Bioturbation is absent throughout the facies.

Interpretation.—This facies is interpreted to comprise coastal-plain and lagoonal deposits due to the high percentage of carbonaceous material in the mudstones, the numerous coal seams and the lack of marginal-marine trace fossils. Vertical tubes are interpreted as root casts and support a vegetated subaerial coastal-plain interpretation (Rahmani 1988). The sheet sandstones are considered to be the deposits of crevasse splays in areas adjacent to active fluvial channels on the coastal-plain.

Tide-Dominated Facies Association

The tide-dominated facies association occurs mainly in the proximal, southwestern parts of the studied exposures. Units of this facies association are erosionally based, which causes variable thickness and lateral extent. Down-dip, the tide-dominated facies are separated from the wave-dominated facies by a basal erosion surface and are locally top truncated by an overlying wave-dominated unit. This facies architecture is described in detail later in the study.

Tidal Channel-Fill Facies (T1)

Description.—This facies is composed of upper fine- to lower medium-grained sandstones, arranged into sets of both trough and planar cross-bedding with carbonaceous siltstone and mudstone drapes along many foresets and toesets (Fig. 3B). Sandstones are well sorted and texturally mature, similar to those of facies W4. Planar cross-bed sets are 0.1–1 m thick, exhibit numerous reactivation surfaces and are oriented in opposite directions (Figs. 3C, 4, 5) in addition to rare herringbone cross-stratification. This facies occurs within channelized sand bodies which are laterally amalgamated into extensive sheets with irregular erosional relief at their bases. Individual channelized bodies range in thickness from 1 to 20 m, and their basal surfaces are lined with rip-up mud clasts, woody debris, and rare shell debris. Low-angle inclined bedding surfaces occur at and parallel to the margins of several channelized bodies. Trace fossils are common, including *Skolithos*, *Thalassinoides*, *Ophiomorpha*, and rare *Teredolites*, which occurs in rafted wood debris. Channelized sandbodies of facies T1 are observed to thin in a paleolandwards direction (southwest) and pinch out against proximal lower-shoreface

deposits (facies W4) at their down-dip terminations. Channels thin gradually up dip over several kilometers, and pinch out within coastal-plain and lagoonal deposits (facies C1).

Interpretation.—The abundance of carbonaceous siltstone and mudstone drapes on cross-bed foresets and toesets implies periodic variations in flow velocity, while bidirectional paleocurrents and herringbone cross-stratification indicate deposition under opposing current directions. In combination, these structures are diagnostic of tidal currents (e.g., Nio and Yang 1991). The occurrence of facies T1 in channelized bodies with inclined bedding surfaces at their margins indicates lateral accretion of migrating channels, to form wider sheet-like bodies. Trace fossils such as *Skolithos*, *Thalassinoides*, and *Ophiomorpha* (while not conclusive), all indicate deposition under high-energy, shallow-marine conditions (Pemberton et al. 1992), while mud clasts and woody debris at sandbody bases implies erosion of a vegetated coastal-plain. The occurrence of this facies up-dip of wave-dominated shoreface deposits (e.g., facies W4) and down-dip of coastal-plain and lagoonal deposits (facies C1) suggests deposition in a mixed wave-tide barrier-island setting, most likely as the fill of tidal inlet channels (Yang and Nio 1985; Fenies and Faugères 1998). The similarity between the textural and grain-size characteristics of sandstone in this facies to that of proximal lower-shoreface sandstones (facies W4) suggests that sediment was supplied from the shoreface and reworked into the tidal channel deposits (Kumar and Saunders 1976).

Tidally Influenced Fluvial Channel-Fill Facies (T2)

Description.—Facies T2 occurs as erosionally based, channelized sandbodies 1–6 m thick characterized by abundant sets and cosets of trough and planar cross-bedding. Sandstones are predominantly fine- to medium-grained, but more rarely lower coarse-grained, and are poorly to moderately sorted. Sandbody bases are lined by lags of pebble-grade mud clasts in addition to abundant plant and woody debris. Cross-sets fine upwards, range in thickness from 0.1 to 1–2 m, and are commonly overlain by ripple-laminated beds. Some are sigmoidal (Fig. 3D). Both single and compound cross-sets contain rare carbonaceous drapes on foresets and toesets, and show bidirectional paleocurrents with a significant majority towards the north-northeast (Fig. 5). Low-angle inclined bedding surfaces parallel to the margins of several channelized bodies are abundant (vertical spacing of 0.2–0.5 m), and can be traced from top to base of the sandbodies that contain them (5–15 m in length). Contorted cross-beds are also commonly observed throughout. Rare *Thalassinoides* and *Skolithos* occur sporadically throughout this facies. Facies T2 occurs only in the lower part of the exposures, and is intimately associated with tidal flat (facies T3) and coastal-plain deposits (facies C1). Where exposed down-dip, units are separated from proximal lower-shoreface deposits (facies W4) by an erosion surface.

Interpretation.—In geometry, sandstone content, and predominant sedimentary structures, this facies appears to have much in common with tidal channel-fill deposits (facies T1). The occurrence of bidirectional cross-sets with carbonaceous drapes on their foresets and toesets indicates a tidal origin (e.g., Nio and Yang 1991). However, trace fossils are significantly less common, implying an environmental stress (Pemberton et al. 1992), possibly related to brackish salinity conditions. The abundance of water-escape structures and contorted cross-bedding implies rapid deposition and high sediment supply. Carbonaceous plant debris and wood fragments are common in the channel bases

and suggest an abundant supply of coastal-plain material in close proximity. The widespread occurrence of inclined bedding surfaces at the margins of channelized sandbodies of facies T2 indicates lateral accretion of migrating channels of sinuous plan form, which is common in both fluvial and fluvial–tidal systems (Nio and Yang 1991).

Tidal Flat Facies (T3)

Description.—This facies consists of intercalated beds and laminae of fine- to medium-grained sandstone, siltstone, and mudstone. Wavy bedding with planar laminae, wave-ripple cross laminae, and ripple cross laminae are common (Fig. 3E), with abundant carbonaceous drapes on both ripple foresets and wave-ripple cross lamination. Bioturbation is sparse, but occasional *Thalassinoides* occur at the base of sand-prone intervals. Root traces are absent throughout this facies. Sandstone and mudstone beds typically do not exceed 0.2 m in thickness but stack vertically into units 1–5 m thick. Facies T3 is observed only in the basal exposures of the Cliff House Sandstone, in association with coastal-plain and lagoonal (facies C1), tidal channel-fill (facies T1), and tidally influenced fluvial channel-fill deposits (facies T2).

Interpretation.—The heterolithic nature of this facies and abundance of carbonaceous drapes on ripple forms are suggestive of deposition under tidal currents (e.g., Nio and Yang 1991). Sparse bioturbation reflects a stressed environment (Pemberton et al. 1992), consistent with a tidal setting (e.g., Fenies and Faugères 1998; Nio and Yang 1991). Given its association with channelized sandstones reflecting tidal influence (facies T1, T2), it seems likely that this facies records deposition on tidal flats that were laterally equivalent to coeval tidal channels (cf. Donselaar and Nio 1982).

Wave-Dominated Facies Association

The wave-dominated facies association occurs mainly in the distal (northeastern) parts of the study area. Typical units of this association are highly continuous along both depositional dip and strike. Up-dip, these units are separated from the tide-dominated facies association by an erosion surface.

Foreshore Facies (W1)

Description.—This facies comprises moderately sorted, upper fine- to medium-grained sandstone arranged into planar-parallel to low-angle ($< 3^\circ$) laminated units that are 1–2 m thick (Fig. 4A). The sandstones are unbioturbated. Units of facies W1 form tabular sheets that can be traced for up to 2 km down depositional dip, which overlie and pass down depositional dip into upper shoreface deposits (facies W2). The facies is typically erosionally overlain by either tidal channel (facies T1) or proximal lower-shoreface (facies W3) deposits.

Interpretation.—The dominant depositional process is interpreted to have been wave swash–backwash action in a foreshore setting, based on the laterally extensive upper-flow-regime bedforms, the association with other wave-dominated facies, and due to the lack of bioturbation (e.g., Clifton et al. 1971).

Upper-Shoreface Facies (W2)

Description.—This facies consists of moderately well-sorted, upper fine- to medium-grained sandstones which are arranged into thin (0.1–0.4 m) trough and planar cross-sets and cosets (Fig. 4B). Units of facies W2 are typically between 1 and 2 m thick. These units gradationally overlie and pass down dip into proximal lower-shoreface deposits

(facies W3), and grade upward into foreshore deposits (facies W1). Bioturbation is sparse (*Skolithos*, *Diplocraterion*).

Interpretation.—Sparse bioturbation by traces that constitute a *Skolithos* ichnofacies indicates deposition in a sand-rich, high-energy shallow-marine setting (Pemberton et al. 1992). Planar and trough cross-bedding records the migration of dunes in response to unidirectional currents; the association of this facies with both proximal lower-shoreface (facies W3) and foreshore deposits (facies W1) strongly suggests deposition under the influence of fair-weather waves on the upper-shoreface and in the inferred environment may be due to onshore-, longshore-, and/or offshore-directed, wave-generated currents (Clifton et al. 1971).

Proximal Lower-Shoreface Facies (W3)

Description.—Facies W3 is composed of amalgamated beds of swaly- and hummocky cross-stratified, well-sorted, fine-grained sandstones (Fig. 4C). Each unit of the facies is dominated by hummocky cross stratification at its base and more common swaly cross stratification at its top. In some locations, swaly cross stratification is observed to pass gradationally upwards into high-angle trough cross-stratification. Rare sets of wave-ripple cross lamination and planar to low-angle lamination are also observed. Bioturbation is common, by a trace-fossil assemblage including abundant *Ophiomorpha nodosa*, *Thalassinoides*, and more rarely *Arenicolites*, *Palaeophycos*, and *Planolites*. Beds commonly have a slightly coarser basal lag, which contains carbonate shell debris, wood fragments, and rare shark teeth. Lags are often overprinted by carbonate-cemented concretions and concretionary horizons. Units of facies W3 form tabular sheets that are 2–8 m thick and laterally continuous along dip and strike for > 10 km. Units grade up dip into and are overlain by upper shoreface deposits (facies W2), and they grade down dip into and overlie distal lower-shoreface deposits (facies W4).

Interpretation.—The dominance of swaly- and hummocky cross-stratification reflects deposition above storm-wave base, where storm oscillatory flows allow aggradation of bedforms under waning flow (Hunter and Clifton 1982). The dominance of swaly-cross stratification is typical of the upper part of the lower-shoreface, while preservation of hummocky cross-stratification is likely to have occurred closer to storm wave base (Dott and Bourgeois 1982; Leckie and Walker 1982). The absence of shale indicates a highly energetic environment in which silt and mud did not settle out of suspension or was eroded by subsequent storm events. The trace-fossil assemblage indicates a setting where high-energy sandy substrates were rapidly but episodically emplaced, resulting in a mixed *Skolithos*–*Cruziana* ichnofacies (Pemberton et al. 1992).

Distal Lower-Shoreface Facies (W4)

Description.—This facies is composed of non-amalgamated beds of well-sorted, very fine- to fine-grained sandstones intercalated with siltstones and mudstones. Sandstone beds contain hummocky cross-stratification with rare wave-ripple lamination, while the siltstones form discontinuous, nearly-horizontal lenses in a mudstone matrix. Bioturbation is pervasive in the mudstone intervals, with trace fossils including *Ophiomorpha*, *Thalassinoides*, *Planolites*, *Palaeophycos*, and *Arenicolites*. This facies forms wedge-shaped units that are traceable for up to 5 km in a down-depositional-dip direction and > 10 km along strike. The facies passes up dip into and is overlain by

proximal lower-shoreface deposits (facies W3), and passes down dip into and overlies offshore shales (facies W5).

Interpretation.—The facies records deposition in an area deeper than the proximal lower-shoreface, which is less energetic and less prone to storm events. Hummocky cross-stratified sandstone beds record deposition above storm wave base, and intercalated siltstone and mudstone beds likely reflect fair-weather deposition. Between storms, pervasive bioturbation in the mudstones records colonization of sand beds in between storms by a mixed *Skolithos*–*Cruziana* ichnofacies (Pemberton et al. 1992).

Offshore Facies (W5)

Description.—Facies W5 comprises interbedded siltstones and mudstones with very rare, very fine- and fine-grained sandstone beds which do not exceed 0.5 m in thickness. These thin sandstone beds occasionally exhibit planar parallel and asymmetric ripple-cross lamination. Several sandstone beds infill steep-sided erosional scours (Fig. 4D). Bioturbation is sparse to moderate in intensity and is dominated by *Planolites*, with rare *Ophiomorpha* and *Thalassinoides*. This facies occurs as low-angle tabular wedges of > 5 km dip extent, and they grade up dip into distal lower-shoreface deposits (facies W4).

Interpretation.—This facies represents deposition beneath mean storm wave base, and represents the most distal facies present in the study area. Major, infrequent storms are recorded by steep-sided, sandstone-filled scours that resemble gutter casts (Myrow 1992) and formed as a result of increased rip currents during the waning storm. Rare *Ophiomorpha* and *Thalassinoides* indicate episodic increases in marine energy and could be either opportunistic or transported down-dip by marine currents. The siltstone and mudstone beds record fair-weather deposition.

Mouth-Bar Facies (D1)

Description.—Facies D1 is locally restricted in its distribution, occurring at two stratigraphic levels. Units of the facies pass laterally into proximal lower-shoreface deposits (W3), and are erosionally truncated by tidal channel-fill deposits (T1) at their up-dip pinchouts, where exposed. Facies D1 comprises interbedded fine-grained sandstones, siltstones, and mudstones. Sandstone units consist of multiple amalgamated beds in southwest–northeast-trending (i.e., approximately shoreline-normal) channels that are 0.9–4 m thick and 10–50 m wide, while intervals of facies D1 are up to 5 m in overall thickness (Fig. 5A, B). Mudstone rip-up clasts are common at the bases of sandstone units, including large (0.2–1.4 m diameter) mudstone “rafts.” Many sandstone beds are hummocky and swaly cross-stratified in their lower part, with current-ripple and wave-ripple cross-laminated tops (Fig. 4E). Other beds contain planar-parallel and low-angle inclined lamination, while thin (0.05–0.10 m) graded sandstone beds (very fine- to fine-grained) with structureless bases and parallel-laminated tops are also present. Siltstones and mudstones contain coal intraclasts, wood fragments, and carbonaceous plant debris. *Ophiomorpha*, *Planolites*, and *Thalassinoides* are common in mudstones, siltstones, and sandstones, while *Teredolites* is also observed in larger wood fragments.

Interpretation.—The localized occurrence of channelized sandstones with intercalated carbonaceous-rich mudstones is interpreted to reflect proximity to a high-energy fluvial input point along strike from, and in water depths similar to, lower-shoreface deposits (facies W3), most likely in mouth bars along a wave-dominated deltaic shoreline (Bhattacharya and Giosan 2003). The erosional base of the sandbody

could also indicate deposition in the terminal distributary channel (Olariu and Bhattacharya 2006; Ahmed et al. 2014). Graded beds in the sandstones are indicative of sediment-gravity-flow deposits, while the hummocky and swaly cross-stratification records reworking by waves during storm events. Bioturbation reflects episodic colonization by a mixed *Skolithos–Cruziana* ichnofacies (Pemberton et al. 1992), most likely in between storms. This facies provides indirect evidence that the studied portion of the paleo-coastline was near to a fluvial input point during deposition of the upper Cliff House Sandstone.

FACIES SUCCESSIONS AND KEY STRATIGRAPHIC SURFACES

Conceptual stratigraphic models of barrier-island depositional systems indicate that a number of surfaces may be generated during transgression, and that these surfaces are arranged in a particular order in a vertical succession (e.g., Swift 1968; Demarest and Kraft 1987; Cattaneo and Steel 2003). In landward locations, the onset of transgression is marked by the drowning of the subaerial coastal-plain and development of a lagoon above a transgressive surface (TS). Landward retreat of the barrier island results in erosion of lagoonal deposits by backstepping tidal inlet channels and associated networks of back-barrier channels that drain through the tidal inlets, creating a tidal ravinement surface (tRS). Continued barrier-island retreat results in erosion by fair-weather and storm waves, generating a wave ravinement surface (wRS), as the shoreface on the seaward side of the barrier passes the location of the vertical succession. Further deepening may occur as the barrier island continues to retreat to its most landward position; the greatest water depths occur at the flooding surface (FS). Thus, four surfaces (TS, tRS, wRS, and FS) may be sequentially generated during a single transgression of a barrier-island depositional system. The surfaces have variable geometry and extent. TS are planar, but their extent mimics that of the overlying, initially developed lagoon. These surfaces form in proximal locations only. tRSs are composite erosion surfaces of highly variable relief and extent, depending on the depth and migration history of tidal channel networks. wRSs are laterally extensive, planar erosion surfaces, reflecting the relatively uniform extent and depth of wave erosion on the shoreface, and steepen near their landward terminations to form paleoseaward-dipping “steps” that represent the paleo-shoreface profile. wRSs are the fundamental surfaces which control the overall preservation of facies tracts; the depth of erosion at each wRS is controlled by the depth of wave base during its creation and the migration and climb (i.e., trajectory) of the surface through time (Swift, 1975; Thorne and Swift, 1991). FSs are extensive, especially in distal locations, and their geometry can reflect the paleo-shelf profile. Some of these surfaces may be coincident with each other, depending on the depth of erosion and volume of deposition.

In the section below, we document the key stratigraphic surfaces in the Cliff House Sandstone dataset, in the context of the facies successions that are juxtaposed across them. Incomplete exposure precludes discrimination of coastal-plain and lagoonal deposits (which are combined as facies C1), such that the TSs cannot be recognized. Both tRSs and wRSs are interpreted, with the latter being coincident with FS in the study area. Wave Ravinement Surfaces (wRS) and Flooding Surfaces (FS)

Description.—Wave-dominated facies are typically arranged in upward-shallowing sandstone tongues that comprise, from deep to shallow: offshore (W5), distal lower-

shoreface (W4), proximal lower-shoreface (W3), upper-shoreface (W2), and foreshore deposits (W1). In any vertical measured section, only part of this complete facies succession is present. Lower-shoreface and offshore deposits (W3–W5) predominate in distal locations (e.g., successions between wRS 800 and 900, wRS 900 and 1000, and wRS 1000 and 1100 in Fig. 6B), but are locally supplemented by mouth-bar deposits (facies D1) (e.g., succession between wRS 700 and 800 in Fig. 6B). Foreshore, upper-shoreface, and proximal lower-shoreface deposits (facies W1–W3) occur in proximal locations, near the up-dip pinchout of a particular wave-dominated sandstone tongue (e.g., succession between wRS 600 and 700 in Fig. 6A).

The base of each upward-shallowing facies succession is typically marked by an erosional surface that is lined with abundant shelly debris and rip-up clasts, in addition to an increase in grain size (e.g., Fig. 7B). Locally, the surface is overprinted by thin carbonate-cemented concretions that may be laterally amalgamated to form a concretionary horizon. The erosion surface may be marked by a series of sharp, steep-sided gutter or scour casts into the underlying deposits, notably which consist of coal or carbonaceous shale (facies C1) (Figs. 4F, 7A). Elsewhere, the surfaces have a planar geometry, and may be associated with intense bioturbation. The erosion surfaces can be traced for > 10 km along strike and for several kilometers down dip (Figs. 8–13). However, where the surfaces juxtapose similar lithologies, commonly proximal lower-shoreface deposits (facies W3), they have only a subtle expression (a bedding break) and are represented by dashed lines in Figs. 10–13. Two styles of up-dip termination of the wRS are observed. First, a surface steepens in a paleolandward direction, to form a concave-upward “step,” which is then truncated by a similar overlying surface (e.g., wRS 100 in Figs. 10, 13). Second, and more commonly, the surface maintains a planar, horizontal geometry and is truncated by an erosion surface at the base of overlying tidal channel-fill deposits (facies T1) (e.g., wRS 200, 400, 500 in Fig. 10; wRS 100, 200, 300, 500, 900 in Fig. 12; wRS 200, 400, 500 in Fig. 13). The deposits directly overlying each erosion surface constitute the most distal facies of the overlying upward-shallowing, wave-dominated facies succession (e.g., offshore facies W5 in the successions above wRS 700 and wRS 900 in Fig. 6B; distal lower-shoreface facies W4 in the succession above wRS 1000 in Fig. 6B; proximal lower-shoreface facies W3 in the succession above wRS 800 in Fig. 6B).

Interpretation.—Each of the erosion surfaces bounding the upward-shallowing, wave-dominated sandstone tongues is interpreted as a wRS, because the occurrence of overlying swaly and hummocky cross-stratified sandstones (facies W3 and W4) implies that wave and/or storm processes generated the surface. This interpretation is supported by the localized occurrence of gutter casts, which formed by deep localized scour of a cohesive substrate by offshore-directed, storm-generated bottom currents (e.g., Myrow 1992). The occurrence of shell material in a lag lining each erosion surface indicates nondeposition due to sediment winnowing, and is characteristic of wRS in other successions (Sixsmith et al. 2008). Carbonate-cemented concretions around the lags are interpreted to be the result of localized redistribution of highly concentrated bioclastic carbonate during early diagenesis.

The occurrence of distal facies directly above each interpreted wRS, without any intervening upward-deepening succession, indicates that wRS are coincident with FS in

the study area. Based on the lateral offset between facies tracts across the wRS and coincident FS (Figs. 10, 12, 13), each surface records an increment of nondepositional shoreline retreat of 3 to > 10 km.

Tidal Ravinement Surfaces (tRS)

Description.—Tidal channel-fill deposits (T1) occur in multistory and/or multilateral bodies that are locally marked by landward dislocations of facies tracts, such that they erosionally overlie coastal-plain and lagoonal deposits (facies C1) (e.g., tRS 400 in Fig. 10; tRS 200, 500, 900, 1100 in Fig. 12; tRS 400, 600 in Fig. 13), or deeply incise into and/or truncate underlying wave-dominated sandstone tongues near their up-dip pinchouts (e.g., tRS 400, 500, 600, 800 in Fig. 10; tRS 200, 300, 500, 600 in Fig. 12; tRS 400, 500, 600 in Fig. 13). Individual channel-fill bodies are 2–5 m thick and 400–1300 m wide. The tidal channel-fill complexes are marked by a composite erosion surface at their bases, lined by a lag of mud rip-up clasts, coal fragments, and woody debris that contains rare *Teredolites* (Fig. 7C, D). These composite erosion surfaces exhibit pronounced relief (up to 12 m), are variably laterally persistent down depositional dip (1–7 km) (Figs. 8, 9, 10, 12, 13), and appear to be correlatable between dip-oriented canyons over strike distances of c. 7 km (compare Figs. 10, 12, 13). The tidal channel-fill complexes that overlie the composite erosion surfaces are truncated at their tops by interpreted wave ravinement surfaces (Figs. 8, 9, 10, 12, 13). Channel-fill complexes thin up dip and break up into individual, disconnected channel-fill bodies encased within carbonaceous shales (facies C1) (Figs. 10, 12, 13).

Interpretation.—Although erosion surfaces at the base of migrating tidal inlets can occur in a range of stratigraphic architectures (e.g., Nichol et al. 1996), two aspects of the context of the erosion surface at the bases of multistory and/or multilateral tidal channel-fill complexes in the study area suggest that they are composite tRSs. First, erosion surfaces characterized by landward dislocations of facies tracts provide direct stratigraphic evidence of shoreline retreat. Second, all of the tidal channel-fill complexes are truncated down depositional dip by an overlying wave ravinement surface (Figs. 10, 12, 13), which suggests that their basal composite erosion surfaces formed mainly during shoreline retreat. This interpretation implies that only the deeper parts of the tidal channel-fill complexes, which have the highest preservation potential, are preserved between the underlying tRS and the overlying wRS.

STRATIGRAPHIC ARCHITECTURE

Ten high-frequency stratigraphic cycles are documented in the Cliff House Sandstone in the study area (wRS 100–200, wRS 200–300, wRS 300–400, wRS 400–500, wRS 500–600, wRS 600–700, wRS 700–800, wRS 800–900, wRS 900–1000, wRS 1000–1100 in Figs. 10–13). Wave ravinement surfaces have been numbered in the stratigraphic order they appear (100 being the oldest, 1100 the youngest). The cross sections presented (Figs. 10–13) have been correlated into a fence panel (Fig. 14), and clear differences can be recognized between the dip and strike architecture. In the strike orientation, facies belts and ravinement surfaces are widely correlatable and show considerable lateral continuity (~ 10 km) in both the up-dip (South Mesa to West Mesa) and down-dip (Gallowash to Pueblo Bonito) regions. In the dip orientation, facies belts display a consistent succession despite separation between facies associations (tide and wave) by erosional surfaces. As such, the facies belts occur in a predictable fashion.

Given the 4 Myr duration of the entire Cliff House Sandstone (Fig. 1B), of which only the upper one third is exposed in Chaco Cultural Natural Historical Park, each high-frequency stratigraphic cycle represents c. 100 kyr. In this section, we describe the internal architecture of these high-frequency stratigraphic cycles (parasequences), and their stacking into larger, low-frequency patterns (parasequence sets) in the context of the overall net-transgressive Cliff House Sandstone succession.

In order to characterize low-frequency patterns, we use shoreline trajectory as a tool. Shoreline trajectory is defined as “the cross-section of the shoreline migration path in the depositional dip direction” (Helland-Hansen and Martinsen 1996), and has been applied by numerous authors to quantify aspects of stratigraphic architecture (Løseth and Helland-Hansen 2001; Løseth et al. 2006; Sixsmith et al. 2008; Hampson et al. 2009; Helland-Hansen and Hampson 2009; Allen and Johnson 2011; Zhu et al. 2012). Shoreline trajectories have been calculated from the positions in successive high-frequency stratigraphic cycles of the up-dip pinchout of wave-dominated deposits, as a proxy for the position of the shoreline during the turnaround from regression to transgression, for the dip-oriented cross sections illustrated in Figures 10 and 13. Where wave-dominated deposits cannot be traced to their up-dip pinchout position, their most paleolandward position in the cross sections has been used instead. Sediment thicknesses were not decompacted, and wRS 600 was used as a paleohorizontal datum surface due to being the most extensive and prominent surface in the exposures. These assumptions are likely to have a relatively small effect on the calculated shoreline trajectories (cf. Hampson et al. 2009).

High-Frequency Stratigraphic Cycles

Each high-frequency stratigraphic cycle records a period of shoreline advance and subsequent retreat. Wave-dominated deposits in each cycle are partitioned into medial-to-distal locations (along the depositional profile), where they define an upward-shallowing, regressive sandstone tongue that is bounded at its top and base by wRS and coincident FS. The proximal shoreline deposits (foreshore and upper-shoreface; W1, W2) are present only in some tongues, implying that such deposits are variably preserved due to erosion at the overlying wRS. Tide-dominated deposits in each cycle are partitioned into proximal locations, as a tidal channel-fill complex (T1) bounded at its base by a tRS and at its top by a wRS and coincident FS. Each tidal channel-fill complex splits and passes paleolandward into undifferentiated coastal-plain and lagoonal deposits (C1) that locally contain tidal channel-fill deposits (T2) and tidal-flat deposits (Facies T3). The detailed architecture of this transition is not resolved in the study dataset, but it appears likely that much of the coastal-plain and lagoonal strata were accumulated during shoreline retreat and deposition of the tidal channel-fill complex with which they interfinger.

Stacking of High-Frequency Stratigraphic Cycles

Patterns in the vertical stacking of high-frequency stratigraphic cycles (cf. parasequence stacking patterns *sensu* Van Wagoner et al. 1990) are defined principally by the position of facies tracts in successive high-frequency stratigraphic cycles along a dip-oriented transect (e.g., Figs. 10, 12, 13, 14). There is little variation in the position of facies tracts in successive high-frequency stratigraphic cycles along depositional strike (e.g., Fig. 11; also by comparison of Figs. 10, 12, 13, 14). Shoreline trajectory is used as a quantitative measure of stacking patterns, and is defined using the positions in

successive high-frequency stratigraphic cycles of the up-dip pinchout of wave-dominated deposits.

Four low-frequency stratigraphic packages (cf. parasequence sets *sensu* Van Wagoner et al. 1990) are identified on the basis of shoreline trajectories and associated stacking patterns of the ten high-frequency stratigraphic cycles. These four packages are described below.

Chaco Unit 1 (below wRS 100)

Description.—Exposures of the basal unit are up to 30 m thick in the southwestern part of the study area (South Mesa; Fig. 2) and the unit passes into the subsurface in its northern part (north of Chaco Canyon; Fig. 2) (e.g., Fig. 10). It comprises tidally influenced fluvial channel-fill deposits (facies T2) which are intercalated with coastal-plain, lagoonal and tidal-flat deposits (facies C1, T3). Laterally and vertically stacked channel-fill deposits occur at two distinct stratigraphic levels that can be correlated for up to 5 km down depositional dip (labeled Tf1 and Tf2 in Fig. 10). Channel-fill bodies become less densely stacked and more isolated both up depositional dip and in stratigraphically higher positions in Chaco Unit 1. Tide-dominated and wave-dominated deposits that are broadly coeval to the stacked channel-fill deposits in the lower part of Chaco Unit 1 are not exposed.

Interpretation.—The lower part of Chaco Unit 1 is interpreted to represent deposition by a network of laterally mobile tidally influenced fluvial channels that drained towards the coastline in the northeast. The upper part of the unit records deposition by similar tidally influenced fluvial channels, although their reduced abundance may reflect more rapid aggradation of the coastal-plain, less frequent river avulsion, and/or a lateral shift in the trunk river to another location. The first major transgression, represented by high-frequency stratigraphic cycle wRS 100–200, occurred at the same time.

Chaco Unit 2 (wRS 100–600)

Description.—Chaco Unit 2 is c. 40 m thick, and comprises five stacked high-frequency stratigraphic cycles (wRS 100–200, wRS 200–300, wRS 300–400, wRS 400–500, wRS 500–600 in Fig. 10). Wave-dominated sandstone tongues in the paleoseaward part of the high-frequency stratigraphic cycles are c. 2–8 m thick. The lower four tongues (wRS 100–200, wRS 200–300, wRS 300–400, wRS 400–500) maintain a uniform thickness along strike (c. 10 km) and down depositional dip (c. 6 km), whereas the uppermost sandstone tongue (wRS 500–600) thins gradually down dip. Foreshore and upper-shoreface deposits (facies W1, W2) are present, but not widespread, in the upper part of only one tongue (wRS 200–300; Figs. 11, 13). Mouth-bar deposits (facies D1) are also present locally in only one tongue (wRS 400–500; Figs. 10, 11, 13). Tidal channel-fill complexes in the four high-frequency stratigraphic cycles are locally stacked vertically to form a thick (up to 30 m), composite sandbody. The paleolandward part of Chaco Unit 2 comprises interstratified coastal-plain deposits (C1) and tidal channel-fill sandbodies (T2).

Interpretation.—Chaco Unit 2 records aggradational to slightly progradational stacking of high-frequency stratigraphic cycles (Fig. 10–14). The scarcity of foreshore and upper-shoreface deposits is attributed to erosion at wRS that truncates the wave-dominated sandstone tongue in each high-frequency stratigraphic cycle. In contrast, the

patchy, localized occurrence of mouth-bar deposits supports the interpretation of a small number (1?) of widely spaced (> 10 km) fluvial sediment-input points along the Chaco Unit 2 shorelines in the study area (Figs. 14, 15A).

Chaco Unit 3 (wRS 600–800)

Description.—Chaco unit 3 is 10–15 m thick in the southwestern part of the study area and thickens to 30–40 m towards the northeast (Figs. 10–13). It comprises two stacked high-frequency stratigraphic cycles (wRS 600–700, wRS 700–800 in Fig. 10). Chaco unit 3 is bounded at its base by wRS 600, which places distal lower-shoreface and offshore deposits (facies W4, W5) directly above the lower-shoreface, tidal channel-fill and coastal-plain deposits (facies W3, T1, C1) of Chaco unit 2. Both overlying wave-dominated sandstone tongues lack foreshore and upper-shoreface deposits (facies W1, W2), but the upper tongue (wRS 700–800) does contain laterally extensive mouth-bar deposits (facies D1) (Figs. 10–13). Only the upper tongue is eroded by tidal channel-fill sandstone complexes, in the southern part of the study area (Figs. 10, 11, 13). Chaco Unit 3 does not contain any deposits of the continental facies association (facies C1) in the study area (Figs. 10–13). In the Weritos Rincon section (Fig. 13) there is a wave ravinement surface (wRS750) which is not traceable into South Mesa or West Mesa. Despite the dislocation of facies from proximal lower-shoreface to offshore shale, this appears to be a localized occurrence. As this appears to have been amalgamated into the surrounding shoreface cycles, it is not treated as an individual shoreface tongue.

Interpretation.—WRS 600 represents the most pronounced facies dislocation across a wRS and coincident FS in the study area (Figs. 10, 12, 16) and the widespread occurrence of distal lower-shoreface and offshore deposits (facies W4, W5) directly above it implies the development of relatively deep water. Above this surface, Chaco Unit 3 records progradational stacking of high-frequency stratigraphic cycles (Fig. 16). The widespread extent of mouth-bar deposits (facies D1) in the wave-dominated sandstone tongue of the upper high-frequency stratigraphic cycle is attributed to the presence of one major or multiple minor, closely spaced fluvial sediment-input points along the Chaco Unit 3 shorelines in the study area.

Chaco Unit 4 (wRS 800–1100)

Description.—Chaco Unit 4 is at least 20–40 m thick and thickens towards the southwest, although its top is not exposed. The unit comprises three stacked high-frequency stratigraphic cycles (wRS 800–900, wRS 900–1000, wRS 1000–1100, in Fig. 10). Thin (< 1 m) intervals of distal lower-shoreface and offshore deposits (facies W4, W5) are present in the lower parts of wave-dominated sandstone tongues in the uppermost cycles (wRS 900–1000, wRS 1000–1100 in Fig. 10). The lowermost sandstone tongue (wRS 800–900) also contains foreshore and upper-shoreface deposits (W1, W2) locally (Figs. 10–13). Mouth-bar deposits (D1) are absent in Chaco Unit 4 in the study area (Figs. 10–13). Coastal-plain, lagoonal, and tidal channel-fill deposits (C1, T2) are present in the paleolandward parts of two high-frequency stratigraphic cycles (wRS 900–1000, wRS 1000–1100) in the study area, but their relationship with sandstone tongues in paleoseaward locations is not exposed (Figs. 10–13).

Interpretation.—Chaco Unit 4 records progradational stacking of its three lower high-frequency stratigraphic cycles, followed by retrogradational stacking of the uppermost high-frequency stratigraphic cycle (Fig. 16). The absence of mouth-bar

deposits (D1) could indicate that fluvial sediment-input points were not present along the Chaco Unit 4 shorelines in the study area. Alternatively, transgressive ravinement could have removed any evidence of fluvial input, which is in part supported by the thin preserved mouth-bar deposits under wRS 500 in Chaco unit 2 (Figs. 10, 13, 14).

Depositional Model

Each cycle comprises an internal facies architecture which can be separated into two parts. Wave-dominated facies (W1–W5, D1) records the advance of a wave-dominated deltaic shoreline with significant storm-wave activity (e.g., Fig. 15A). The tide-dominated deposits and the composite erosion surfaces at their bases cannot be readily explained by invoking a strandplain or wave-dominated deltaic depositional model (e.g., Fig. 15A). Instead, each tidal channel-fill complex can be accounted for by the retreat of a network of tidal inlets and contiguous back-barrier channels, which represent the preserved remnant of a barrier-island shoreline of mixed wave and tide influence (Fig. 15B).

Facies partitioning in each high-frequency stratigraphic cycle reflects partitioning of regressive and transgressive deposits into the paleoseaward and paleolandward parts of the cycle, respectively. Such partitioning has been widely interpreted in similar stratigraphic cycles (e.g., Cross and Lessenger 1998; Sixsmith et al. 2008; Allen and Johnson 2011). Facies partitioning into different components of a stratigraphic cycle may reflect temporal variations in the depositional-process regime operating along the paleocoastline, with fluvial influence occurring predominantly during regression and tidal influence being enhanced during transgression (cf. Yoshida et al. 2007; Ainsworth et al. 2008, 2011). However, our interpretation also implies that preservation of facies tracts differed over the duration of a stratigraphic cycle, such that there is a strong preservational bias towards wave-dominated-shoreface deposits during regression. Similar wave-dominated shorefaces are inferred to have been present during transgression (on the seaward side of the barrier island), but these facies were not preserved as transgression proceeded, as the sediment was reworked into the back-barrier by tidal processes and eventually eroded by the migrating storm wave base. Overall, we envisage the Cliff House Sandstone depositional system to have had mixed wave, tide, and localized fluvial influence (e.g., “wtf” in the classification scheme of Ainsworth et al. 2011), but individual cycles oscillate between “Wt” (during regression) and “Tf” (during transgression).

Comparison with Other Net-Transgressive Successions

The overall net-transgressive shoreline trajectory for the Cliff House Sandstone in Chaco Cultural Natural Historical Park (from wRS 100 to wRS 1100; Fig. 15) is calculated to be 0.53° . This value is comparable to those of the net-transgressive Hosta Sandstone (0.38° ; Sixsmith et al. 2008) and the middle, net-transgressive part of the John Henry Member (0.41° , Allen and Johnson 2011). These three net-transgressive successions thus share similar quantitative stacking patterns of high-frequency stratigraphic cycles. However, the dip extent of wave-dominated sandstone tongues in high-frequency stratigraphic cycles (cf. parasequences) in the studied Cliff House Sandstone succession is greater (5 to > 10 km) than the dip extent of tongues of similar thickness (2–20 m) and facies composition in the Hosta Sandstone (3.5 to > 6 km, Sixsmith et al. 2008). Wave-dominated sandstone tongues in high-frequency stratigraphic

cycles in the John Henry Member are thicker (15–50 m) and their dip extents are poorly constrained (> 4 km, the length of dip-oriented cross sections, Allen and Johnson 2011).

The differing dip extent of wave-dominated sandstone tongues in the Cliff House Sandstone and Hosta Sandstone is attributable, at least in part, to differences in shoreline trajectory in high-frequency stratigraphic cycles. Regressive and transgressive shoreline trajectories in high-frequency stratigraphic cycles (cf. parasequences) are generally low (< 0.6°; Helland-Hansen and Hampson 2009). In the wRS 700–800 and wRS 800–900 sandstone tongues of the Cliff House Sandstone, regressive shoreline trajectories are very low (c. 0.04°) and corresponding transgressive shoreline trajectories are even lower (< 0.01°). Comparable values for regressive and transgressive shoreline trajectories in the high-frequency stratigraphic cycles of the Hosta Sandstone are up to 0.24° and 0.05–0.29°, respectively (Sixsmith et al. 2008). The lower values of regressive and transgressive shoreline trajectories, and larger dip extents of wave-dominated sandstone tongues, in the Cliff House Sandstone are attributed to relatively high sediment supply as a result of direct fluvial sediment input to deltaic mouth bars (D1) during regression (Fig. 15A). In contrast, the Hosta Sandstone had no direct fluvial sediment input, but was instead supplied only by wave-generated longshore currents (Sixsmith et al. 2008). As a result, it can be inferred that the Cliff House Sandstone shorelines underwent greater progradation in the high-frequency stratigraphic cycles. A similar sediment-supply control on the magnitude of high-frequency shoreline migration is observed in the physical experiments of Kim et al. (2006). It could be postulated that autocyclic variations in the fluvial input to the Cliff House Sandstone coastline would result in periods of abandonment and transgression as sediment supply was unable to keep pace with relative sea-level rise. Alternatively, each cycle of progradation and transgression could be the result of changes in the rate of relative sea-level change (e.g., between accelerating and decelerating rates of sea-level rise) and with a uniform sediment supply.

The order-of-magnitude difference in regressive and transgressive shoreline trajectories in high-frequency stratigraphic cycles (cf. parasequences) in the Cliff House Sandstone and Hosta Sandstone results in significant differences in the connectedness of wRS in the two units. In the Hosta Sandstone, each wRS steepens near its up-dip termination to define a “step” geometry that is truncated by (and thus connected to) an overlying wRS. The paleolandward parts of these wRS are characterized by sandstone-on-sandstone contacts between the underlying and overlying wave-dominated sandstone tongues. In the Cliff House Sandstone, wRS above and below each wave-dominated sandstone tongue are generally unconnected (i.e., there is a greater degree of “step up” between successive wRS than in the Hosta Sandstone; cf. Swift et al. 1991). Offshore shales are more common and have greater dip extents above the wRS, which serves to reduce the proportion of sandstone-on-sandstone contacts between the underlying and overlying wave-dominated sandstone tongues.

Analysis of net-transgressive systems has demonstrated that significant sandbody thicknesses can be preserved (Olsen et al. 1999; Allen and Johnson 2011) given the right conditions of shoreline migration during regressive–transgressive cycles. Of further importance is the preferential preservation of facies types which form the greater part of the rock record in these systems. In this study, the predominant facies types comprise proximal lower-shoreface (W3) and tidal channel-fill (T1). In the most distal log section

in the study area, facies W3 comprises 80% of the preserved facies type, while even in the most proximal position, facies T1 still comprises 40% of preserved facies. Overall 52% of the total preserved facies types, (< 90% of the preserved shallow marine facies types) are W3 and T1. Similar preferential preservation can be observed in other transgressive studies (Sixsmith et al. 2008; Allen and Johnson 2011) but these examples share comparable shoreline-trajectory values (despite different net thickness and length scales) and removes the possibility of identifying any critical threshold values for the shoreline trajectory and facies preservation.

Martinsen and Helland-Hansen (1995) identified that shoreface, barrier-island, and beach systems tend to exhibit along-strike variability on a larger scale when compared with deltaic or estuarine systems. The Cliff House Sandstone and the Hosta Sandstone are two examples of shoreface systems with a variable fluvial input, but along-strike continuity and lateral extent of the facies belts remains comparable. Despite the apparent proximity of fluvial input in the Cliff House Sandstone, there is little along-strike facies variability (on the scale of the area studied). This implies that relative wave strength was strong enough to rework the fluvial input and restrict the likelihood of point-source development (Bhattacharya and Giosan 2003).

CONCLUSIONS

The Cliff House Sandstone records a prolonged period of shoreline retreat during the Late Cretaceous in the Western Interior Seaway. Its internal architecture has proved to be complex, though facies partitioning in each parasequence displays a predictable pattern. Detailed facies mapping has enabled down-dip wave-dominated facies to be traced up-dip into their tide-dominated and continental counterparts. Wave-dominated facies developed during strandplain progradation, during periods of increased sediment supply and relatively low rates of sea-level rise. In contrast, tide-dominated and continental coastal-plain sediments are interpreted to have been deposited in a transgressive barrier-island setting, where net movement of sediment is from the shoreface into the back-barrier. This likely corresponds to a reduced sediment supply from a point source, and the rate of relative sea-level rise is greater. Wave and tidal ravinement surfaces have enabled genetically related packages to be correlated and to be related to periods of regression and transgression. In contrast to models presented for regressive shorelines, the migration of these ravinement surfaces is crucial in determining the preservation and accumulation of depositional facies in transgressive systems. Each tidal ravinement surface can be traced down-dip into a linked wave ravinement surface, and the preservation of back-barrier deposits is reliant on sediments being placed above the tidal ravinement surface but below the wave ravinement surface when it steps up and retreats during ongoing transgression. The amount of sediment supplied during the regressive phase appears to be a crucial factor in determining the separation between each high-frequency cycle and its ravinement surfaces. The Cliff House Sandstone is an example whereby sandstone tongues are disconnected due to a greater step-up in the wave ravinement surface, and this has important connotations in establishing a successful correlation framework.

ACKNOWLEDGEMENTS

This research was supported by project sponsors BP, Chevron, Shell, and the UK Department of Trade and Industry. In particular, we thank Bryan Bracken, David Allsop, Philip Hirst, and Laura Banfield for their input. Fieldwork was conducted under permit

on the Chaco Culture National Historical Park, and we thank Brad Shattuck, Donne Smith, and Tom Lyttle for their invaluable assistance in permitting fieldwork logistics and organization. We are grateful for field assistance from Patrick Dowey, Amy Whitchurch, and Theresa Lloyd. We thank Peter Sixsmith, Yangyang Li, and Janok Bhattacharya for their thorough reviews and editorial comments, which greatly contributed to the clarity of the manuscript.

REFERENCES

- Ahmed, S., Bhattacharya, J.P., Garza, D.E., and Li, Y., 2014, Facies architecture and stratigraphic evolution of a river-dominated delta front, Turonian Ferron Sandstone, Utah, USA: *Journal of Sedimentary Research*, v. 84, p. 97–121.
- Ainsworth, R.B., Flint, S.S., and Howell, J.A., 2008, Predicting coastal depositional style: influence of basin morphology and accommodation to sediment supply ratio within a sequence stratigraphic framework, *in* Hampson, G.J., Steel, R.J., Burgess, P.M., and Dalrymple, R.W., eds., *Recent Advances in Models of Siliciclastic Shallow-Marine Stratigraphy*: SEPM, Special Publication 90, p. 237–263.
- Ainsworth, R.B., Vakarelov, B.K., and Nanson, R.A., 2011, Dynamic spatial and temporal prediction of changes in depositional processes on clastic shorelines: toward improved subsurface uncertainty reduction and management: *American Association of Petroleum Geologists, Bulletin*, v. 95, p. 267–297.
- Allen, J.L., and Johnson, C.L., 2011, Architecture and formation of transgressive–regressive cycles in marginal marine strata of the John Henry Member, Straight Cliffs Formation, Upper Cretaceous of Southern Utah, USA: *Sedimentology*, v. 58 p. 1486–1513.
- Belknap, D.F., and Kraft, J.C., 1981, Preservation potential of transgressive coastal lithosomes on the US Atlantic shelf: *Marine Geology*, v. 42 p. 429–442.
- Bhattacharya, J.P., and Giosan, L., 2003, Wave-influenced deltas: geomorphological implications for facies reconstruction: *Sedimentology*, v. 50, p. 187–210.
- Cattaneo, A., and Steel, R., 2003, Transgressive deposits: a review of their variability: *Earth Science Review*, v. 62, p. 187–228.
- Clifton, H.E., Hunter, R.E., and Phillips, L., 1971, Depositional structures and processes in the non-barred high-energy nearshore: *Journal of Sedimentary Petrology*, v. 41, p. 651–670.
- Cross, T.A., and Lessenger, M.A., 1998, Sediment volume partitioning: rationale for stratigraphic model evaluation and high-resolution stratigraphic correlation, *in* Gradstein, F.M., Sandvik, K.O., and Milton, N.J., eds., *Sequence Stratigraphy: Concepts and Application*: Norwegian Petroleum Society, Special Publication 8, p. 171–195.
- Curry, J., 1964, Transgressions and regressions, *in* Miller, R., ed., *Papers in Marine Geology*: New York, Macmillan, p. 175–203.
- Demarest, J.M., and Kraft, J.C., 1987, Stratigraphic record of Quaternary sea levels: implications for more ancient strata, *in* Nummedal, D., Pilkey, O.H., and Howard, J.D., eds., *Sea-Level Fluctuations and Coastal Evolution*: SEPM, Special Publication 41, p. 223–239.
- Donselaar, M.E., 1989, The Cliff House Sandstone, San Juan Basin, New Mexico: Model for the stacking of “transgressive” barrier complexes: *Journal of Sedimentary Petrology*, v. 59, p. 13–27.

- Donselaar, M.E., and Nio, S.D., 1982, An Eocene tidal inlet washover type barrier-island complex in the South Pyrenean marginal basin, Spain: *Geologie en Mijnbouw*, v. 61, p. 343–353.
- Dott, R.H., and Bourgeois, J., 1982, Hummocky stratification: significance of its variable bedding sequences: *Geological Society of America, Bulletin*, v. 938, p. 663–680.
- Fenies, H., and Faugères, J.C., 1998, Facies and geometry of tidal channel-fill deposits Arcachon Lagoon, SW France: *Marine Geology*, v. 150, p. 131–148.
- Hampson, G.J., and Howell, J.A., 2005, Sedimentological and geomorphic characterization of ancient wave-dominated shorelines: examples from the Late Cretaceous Blackhawk Formation, Book Cliffs, Utah, *in* Giosan, L., and Bhattacharya, J.P., eds., *River Deltas: Concepts, Models, and Examples: SEPM Special Publication 83*, p. 133–154.
- Hampson G.J., Sixsmith, P.J., Kieft, R.L., Jackson, C.A.-L., and Johnson, H.D., 2009, Quantitative analysis of net-transgressive shoreline trajectories and stratigraphic architectures: mid-to-late Jurassic of the North Sea Rift Basin: *Basin Research*, v. 21, p. 528–558.
- Helland-Hansen, W., and Hampson, G.J., 2009., Trajectory analysis: concepts and applications: *Basin Research*, v. 21, p. 454–483.
- Helland-Hansen, W., and Martinsen, O.J., 1996 Shoreline trajectory and sequences: description of variable depositional-dip scenarios: *Journal of Sedimentary Research*, v. 66 p. 670–688.
- Hunter, R.E., and Clifton, H.E., 1982, Cyclic deposits and hummocky cross-stratification of probable storm origin in Upper Cretaceous rocks of Cape Sebastian area, southwestern Oregon: *Journal of Sedimentary Petrology*, v. 52, p. 127–144.
- Kim, W., Paola, C., Voller, V.R., and Swenson, J.B., 2006, Experimental measurement of the relative importance of controls on shoreline migration: *Journal of Sedimentary Research*, v. 762, p. 270–283.
- Krystinik, L.F., and DeJarnett, B.B., 1995, Lateral variability of sequence stratigraphic framework in the Campanian and lower Maastrichtian of the Western Interior Seaway, *in* Van Wagoner, J.C., and Bertram, G.T., eds., *Sequence Stratigraphy of Foreland Basin Deposits: Outcrop and Subsurface Examples from the Cretaceous of North America: American Association of Petroleum Geologists, Memoir 64*, p. 11–26.
- Kumar, N., and Sanders, J.E., 1976, Characteristics of shoreface storm deposits: modern and ancient examples: *Journal of Sedimentary Petrology*, v. 46 p. 145–162.
- Leckie, D.A., and Walker, R.G., 1982, Storm- and tide-dominated shorelines in Cretaceous Moosebar–Lower Gates interval: outcrop equivalents of Deep Basin gas trap in western Canada: *American Association of Petroleum Geologists, Bulletin*, v. 662, p. 138–157.
- Løseth, T.M., and Helland-Hansen, W., 2001, Predicting the pinchout distance of shoreline tongues: *Terra Nova*, v. 13, p. 241–248.
- Løseth, T.M., Steel, R.J., Crabaugh, J.P., and Schellpeper, M., 2006, Interplay between shoreline migration paths, architecture and pinchout distance for siliciclastic shoreline tongues: evidence from the rock record: *Sedimentology*, v. 53, p. 735–767.
- Liu, S., and Nummedal, D., 2004, Late Cretaceous subsidence in Wyoming: Quantifying the dynamic component: *Geology*, v. 325, p. 397–400.

- Miller, K.G., Kominz, M.A., Browning, J.V., Wright, J.D., Mountain, G.S., Katz, M.E., and Pekar, S.F., 2005, The Phanerozoic record of global sea-level change: *Science*, v. 310, p. 1293–1298.
- Molenaar, C.M., 1983, Major depositional cycles and regional correlations of Upper Cretaceous rocks, southern Colorado Plateau, and adjacent area, *in* Reynolds, M.W., and Dolly, E.D., eds., *Mesozoic Paleogeography of West-Central United States: SEPM, Rocky Mountain Section, Symposium Volume*, p. 201–224.
- Myrow, P.M., 1992, Pot and gutter casts from the Chapel Island Formation, southeast Newfoundland: *Journal of Sedimentary Petrology*, v. 62, p. 992–1007.
- Nichol, S.L., Boyd, R., and Penland, S., 1994, Stratigraphic response of wave-dominated estuaries to different relative sea-level changes and sediment supply histories: Quaternary case studies from Nova Scotia, Louisiana, and Eastern Australia, *in* Dalrymple, R.W., Boyd, R., and Zaitlin, B.A., eds., *Incised Valley Systems: Origin and Sedimentary Sequences: SEPM, Special Publication 51*, p. 266–283.
- Nio, S.D., and Yang, C.S., 1991, Diagnostic attributes of clastic tidal deposits: a review, *in* Smith, D., Reinson, G.G.E., Zaitlin, B.A., and Rahmani, R.A., eds., *Clastic Tidal Sedimentology: Canadian Society of Petroleum Geologists, Memoir 16*, p. 3–27.
- Olariu, C., and Bhattacharya, J.P., 2006, Terminal distributary channels and delta front architecture of river-dominated delta systems: *Journal of Sedimentary Research*, v. 76, p. 212–233.
- Olsen, T.R., Mellere, D., and Olsen, T., 1999, Facies architecture and geometry of landward stepping shoreface tongues: the Upper Cretaceous Cliff House Sandstone Mancos Canyon, south west Colorado: *Sedimentology*, v. 46, p. 603–625.
- Palmer, J.J., and Scott, A.J., 1984, Stacked shoreline and shelf sandstone of La Ventana Tongue, Campanian, northwestern New Mexico: *American Association of Petroleum Geologists, Bulletin* v. 68, p. 74–91.
- Pang, M., and Nummedal, D., 1995, Flexural subsidence and basement tectonics of the Cretaceous Western Interior basin, United States: *Geology*, v. 23, p. 173–176.
- Pemberton, S.G., MacEachern, J.A., and Frey, R.W., 1992, Trace fossil facies models: environmental and allostratigraphic significance, *in* Walker, R.G., and James, N.P., eds., *Facies Models: Response to Sea Level Change: Geological Association of Canada*, p. 47–72.
- Rahmani, R.A., 1988, Estuarine tidal channel and nearshore sedimentation of a Late Cretaceous epi-continental sea, Drumheller, Alberta, Canada, *in* de Boer, P.L., van Gelder, A., and Nio, S.D., eds., *Tide-Influenced Sedimentary Environments and Facies: Berlin, Springer*, p. 433–471.
- Rodriguez, A.B., Fassell, M.L., and Anderson, J.B., 2001, Variations in shoreface progradation and ravinement along the Texas Coast, Gulf of Mexico: *Sedimentology* v. 48, p. 837–853.
- Scott, G.R., O’Sullivan, R.B., and Weide, D.L., 1984, Geologic map of the Chaco Culture National Historical Park, north western New Mexico: U.S. Geological Survey Miscellaneous Investigations Series, Map I-1571, 1 sheet, scale 1:50,000.
- Sixsmith, P.J., Hampson, G.J., Gupta, S., Johnson, H.D., and Fofana, J.J., 2008, Facies architecture of a transgressive sandstone reservoir analogue: the Cretaceous Hosta

Sandstone, New Mexico, USA: American Association of Petroleum Geologists, Bulletin, v. 92 p. 513–547.

Swift, D.J.P., 1968, Coastal erosion and transgressive stratigraphy: *Journal of Geology*, v. 76, p. 444–456.

Swift, D.J.P., 1975, Barrier-Island genesis: evidence from the central Atlantic shelf, eastern U.S.A: *Sedimentary Geology*, v. 14, p. 1–43.

Swift, D.J.P., Phillips, S., and Thorne, J.A., 1991, Sedimentation on continental margins: IV. Lithofacies and depositional systems, *in* Swift, D.J.P., Oertel, G.F., Tillman, R.W., and Thorne, J.A., eds., *Shelf Sand and Sandstone Bodies: Geometry, Facies and Sequence Stratigraphy*: International Association of Sedimentologists, Special Publication 14, p. 89–152.

Tamura, T., Saito, Y., and Masuda, F., 2008, Variation in architecture of the Holocene to modern prograding shoreface along the Pacific coast of eastern Japan, *in* Hampson, G.J., Steel, R.J., Burgess, P.M., and Dalrymple, R.W., eds., *Recent advances in models of siliciclastic shallow-marine stratigraphy: SEPM, Special Publication 90*, p. 191–205.

Thorne, J.A., and Swift, D.J.P., 1991, Sedimentation on continental margins, VI: a regime model for depositional sequences, their component systems tracts, and bounding surfaces *in* Swift, D.J.P., Oertel, G.F., Tillman, R.W., and Thorne, J.A., eds., *Shelf Sand and Sandstone Bodies: Geometry, Facies and Sequence Stratigraphy*: International Association of Sedimentologists, Special Publication 14, p. 189–255.

Van Wagoner, J.C., Mitchum, R.M., Campion, K.M., and Rahmanian, V.D., 1990, *Siliciclastic Sequence Stratigraphy in Well Logs, Cores, and Outcrops*: American Association of Petroleum Geologists, Methods in Exploration Series 7, p. II–55.

Yang, C.S., and Nio, S.D., 1985, The estimation of palaeohydrodynamic processes from subtidal deposits using time series analysis methods: *Sedimentology*, v. 32, p. 41–57.

Yoshida, S., Steel, R.J., and Dalrymple, R.W., 2007, Changes in depositional processes: an ingredient in a new generation of sequence-stratigraphic models: *Journal of Sedimentary Research*, v. 77, p. 447–460.

Zhu, Y., Bhattacharya, J.P., Weigo, L., Lapen, T.J., Jocha, B.R., and Singer, B.S., 2012, Milankovitch-scale sequence stratigraphy and stepped forced regressions of the Turonian Ferron Notom deltaic complex, south-central Utah, USA: *Journal of Sedimentary Research*, v. 82, p. 723–746.

Received 22 March 2015; accepted 18 August 2016.

FIGURE CAPTIONS

FIG. 1.—**A**) Schematic paleogeographic reconstruction of the southwestern Western Interior Seaway during Late Cretaceous times, including the approximate location of the Cliff House Sandstone shoreline (Molenaar 1983; Donselaar 1989), the line of cross section (Part B), and the location of the study area (Fig. 2). **B**) Summary chronostratigraphic diagram for the Cretaceous San Juan Basin, New Mexico and Colorado, USA (adapted from the regional cross-sections of Molenaar 1983). Cretaceous stages and approximate ages (in Ma) are indicated. The upper part of the Cliff House Sandstone, which is exposed in Chaco Cultural Natural Historical Park (Fig. 2) is highlighted.

FIG. 2.—Map showing outcrop extent and dataset collected for the Cliff House Sandstone within the Chaco Cultural Natural Historical Park study area. The locations of the

measured sections in Figure 5, architectural panels and photopanoramas in Figures 6, 8, and 9, and correlation panels in Figures 10, 11, 12, and 13 are shown.

FIG. 3.—Photographs of selected facies from the continental and tide-dominated facies associations (Table 1), illustrating diagnostic features: **A**) interbedded carbonaceous mudstones, siltstones, and fine-grained sandstones (facies C1); **B**) carbonaceous shale drapes along the rippled toesets of cross-beds in channelized, tidal inlet sandstone (facies T1); **C**) bidirectional trough cross-bedding in channelized, tidal inlet sandstone (facies T1); **D**) stacked sigmoidal cross-sets, with thin carbonaceous drapes lining some foresets, in tidally influenced fluvial channel-fill unit (facies T2); **E**) rippled sandstone beds and carbonaceous mudstones in wavy-bedded heterolithic, tidal flat deposits (facies T3); and **F**) *Diplocraterion* and *Skolithos* at top of a tide-dominated facies succession, indicating colonization during depositional hiatus. Notebook, lens cap, and pencil for scale in the various photographs.

FIG. 4.—Photographs of selected facies from the wave-dominated facies associations (Table 1), illustrating diagnostic features: **A**) meter-thick unit of planar-parallel-laminated, fine- to medium-grained sandstone deposited under upper-flow-regime conditions (facies W1); **B**) planar cross-set in well-sorted, fine- to medium-grained sandstone (facies W2); **C**) amalgamated beds of swaley cross-stratified, fine-grained sandstone (facies W3); **D**) fine-grained sandstone infilling gutter casts within offshore shales (facies W5); **E**) ripple cross-lamination at the top of a channelized sandstone unit dominated by hummocky and swaley cross-stratification (facies D1; note lens cap in top left for scale), and **F**) meter-scale gutter casts infilled by hummocky cross-stratified and parallel-laminated, fine-grained sandstone (facies W3), and scoured into carbonaceous mudstones and siltstones (facies C1) at a wave ravinement surface. Rucksack, lens cap, and pencil for scale in the various photographs.

FIG. 5.—**A**) Dip-oriented architectural panel and **B**) strike-oriented photopanorama and architectural panel of mouth bar deposits (facies D1) in Gallowash (Figs. 2, 10).

Channelized sandbodies are composed principally of fine-grained sandstones with basal lags of abundant mudstone rip-up clasts.

FIG. 6.—Representative measured sections through the Cliff House Sandstone illustrating facies successions and key stratigraphic surfaces in **A**) a proximal setting, at South Mesa, and **B**) a distal setting, at Gallowash. The locations of the two sections are shown in Figures 2 and 10. **C**) Paleocurrent data for tidal channel-fill (facies T2) and tidally influenced fluvial channel-fill deposits (facies T3) are compiled from locations throughout the study area.

FIG. 7.—Photographs illustrating the character of key stratigraphic surfaces. **A**) Wave and tidal ravinement surfaces within the Weritos Rincon (Fig. 2). Multiple steep-sided scours give the wave ravinement surface a highly irregular geometry. **B**) Detail of wave ravinement surface marked by lag of shell debris. **C**) Abundant woody debris lining tidal ravinement surface at the base of tidal channel-fill deposits (facies T1). **D**) Mud rip-up clasts of irregular geometry near the base of tidal channel-fill deposits (facies T1), and indicating erosion by tidal ravinement.

FIG. 8.—Original and interpreted photopanoramas illustrating vertical stacking of wave-dominated tongues (proximal lower-shoreface deposits; facies W4 identified by “Sf”) and tidal channel-fill complexes (facies T1 identified by “Tc”) within the Cliff House

Sandstone. Each tongue and complex is bounded above and below by wave and tidal ravinement surfaces (wRS, tRS). The photopanorama is oriented along depositional dip and was taken from the southeastern face of South Mesa (Figs. 2, 10). Key to colors for facies and stratigraphic surfaces is as in Figure 10.

FIG. 9.—Original and interpreted photopanoramas illustrating multistory, multilateral nature of tidal channel-fill complexes (facies T1), which are stacked vertically with wave-dominated tongues (proximal lower-shoreface deposits; facies W4). Tidal channel-fill deposits contain prominent sets of lateral accretion surfaces. The photopanorama is oriented along depositional dip and was taken from the southeastern face of West Mesa (Figs. 2, 12). Key to colors for facies and stratigraphic surfaces is as in Figure 10.

FIG. 10.—Correlation panel through a depositional dip profile from South Mesa (southwest; paleolandward) to Gallowash (northeast; paleoseaward) through the Cliff House Sandstone in Chaco Canyon Natural Historical Park (Fig. 2). The datum for the profile is the most widespread transgressive surface, wRS 600. The locations of the measured sections in Figure 5 are shown.

FIG. 11.—Correlation panel through a depositional strike section along northeastern Chaco Canyon, from northwest (paleolandward) to southeast (paleoseaward) (Fig. 2). The datum for the profile is the most widespread transgressive surface, wRS 600.

FIG. 12.—Correlation panel through a depositional dip profile along West Mesa, from southwest (paleolandward) to northeast (paleoseaward), through the Cliff House Sandstone in Chaco Canyon Natural Historical Park (Fig. 2). The datum for the profile is the most widespread transgressive surface, wRS 600.

FIG. 13.—Correlation panel through a depositional dip profile from Weritos Rincon, from southwest (paleolandward) to northeast (paleoseaward), through the Cliff House Sandstone in Chaco Canyon Natural Historical Park (Fig. 2). The datum for the profile is the most widespread transgressive surface, wRS 600.

FIG. 14.—Simplified fence panel illustrating the 3D control offered by the dip- and strike-oriented cross sections. Note the differences in lateral continuity of the facies belts in both a dip- and strike orientation.

FIG. 15.—Depositional model for evolution of the Cliff House Sandstone coastline in the study area. **A**) During the regressive part of each high-frequency stratigraphic cycle, a wave-dominated delta and flanking strandplains that were supplied by longshore currents built out across the shelf. **B**) During the transgressive part of each high-frequency stratigraphic cycle, the landward migration of a barrier island system generated an erosive wave ravinement surface and tidal ravinement surface. Tidal channel-fill and coastal-plain deposits accumulated landward of the retreating barrier.

FIG. 16.—Simplified stratigraphic summary for **A**) the South Mesa and **B**) Weritos Rincon exposures of the Cliff House Sandstone in Chaco Canyon Natural Historical Park, illustrating the stacking patterns of high-frequency stratigraphic cycles (cf. parasequences) and associated shoreline trajectories. Shoreline trajectories are calculated from the positions in successive high-frequency stratigraphic cycles of the up-dip pinchout of wave-dominated deposits, for the dip-oriented cross-sections. Sediment thicknesses are not decompacted and wRS 600 is used as a paleohorizontal datum surface in our calculations of shoreline trajectory. **C**) A conceptual model for the accumulation and preservation of high-frequency cycles (cf. parasequences). Each cycle of shoreface or

tidal accumulation is subject to subsequent erosion by either tidal or wave ravinement, which reworks the upper portion of the cycle resulting in a significantly truncated rock record. The migration of these surfaces in relation to the accumulated facies is therefore crucial to understanding the preservation potential of each cycle.

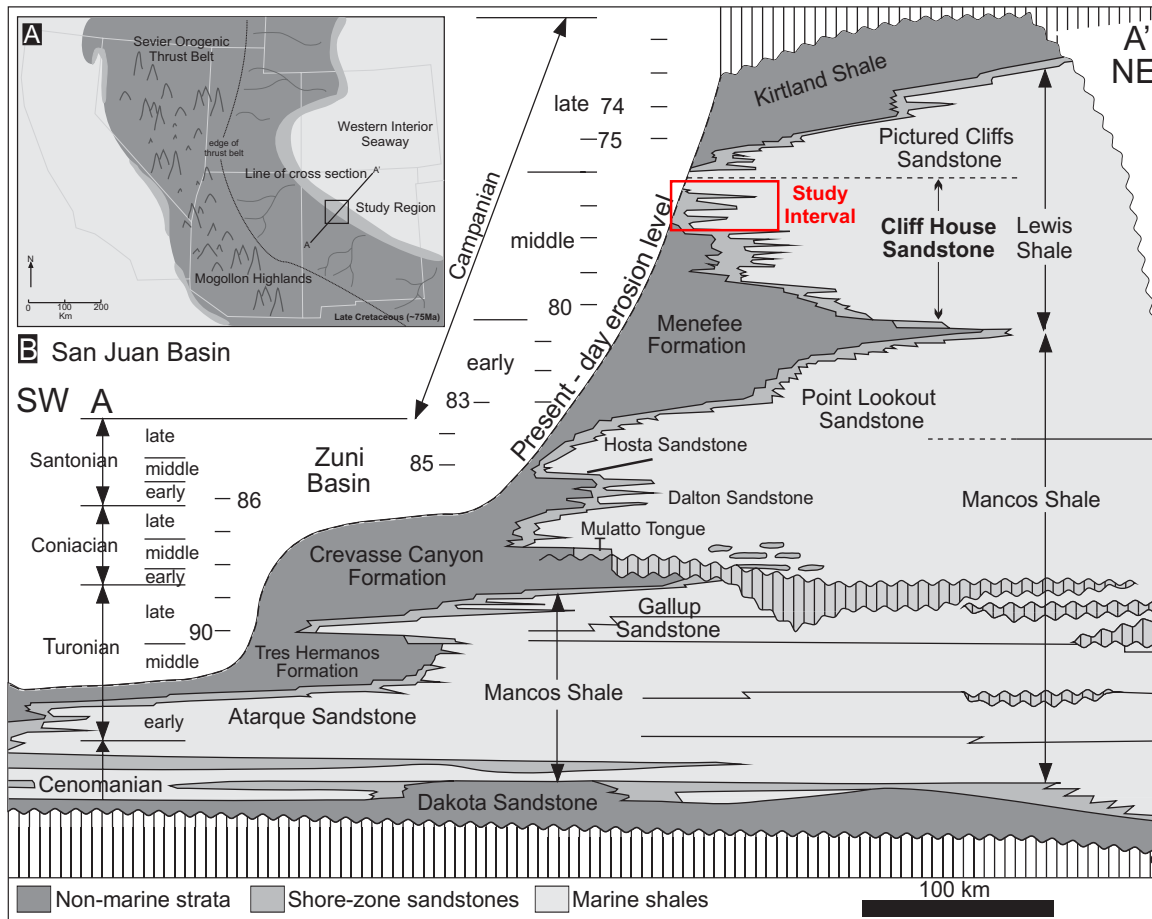


Figure 1

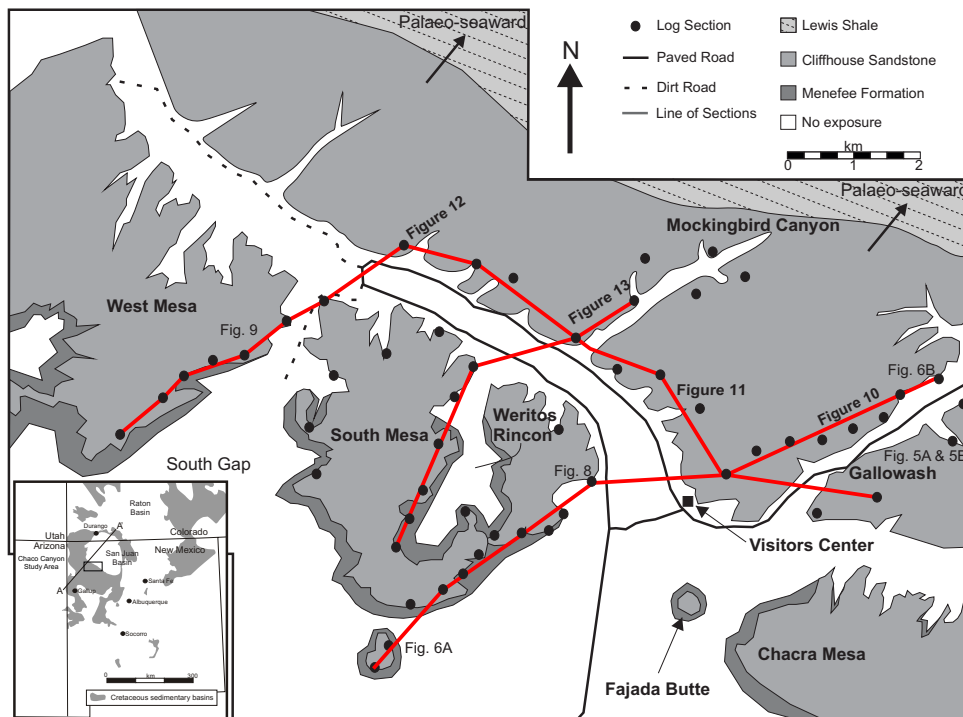


Figure 2

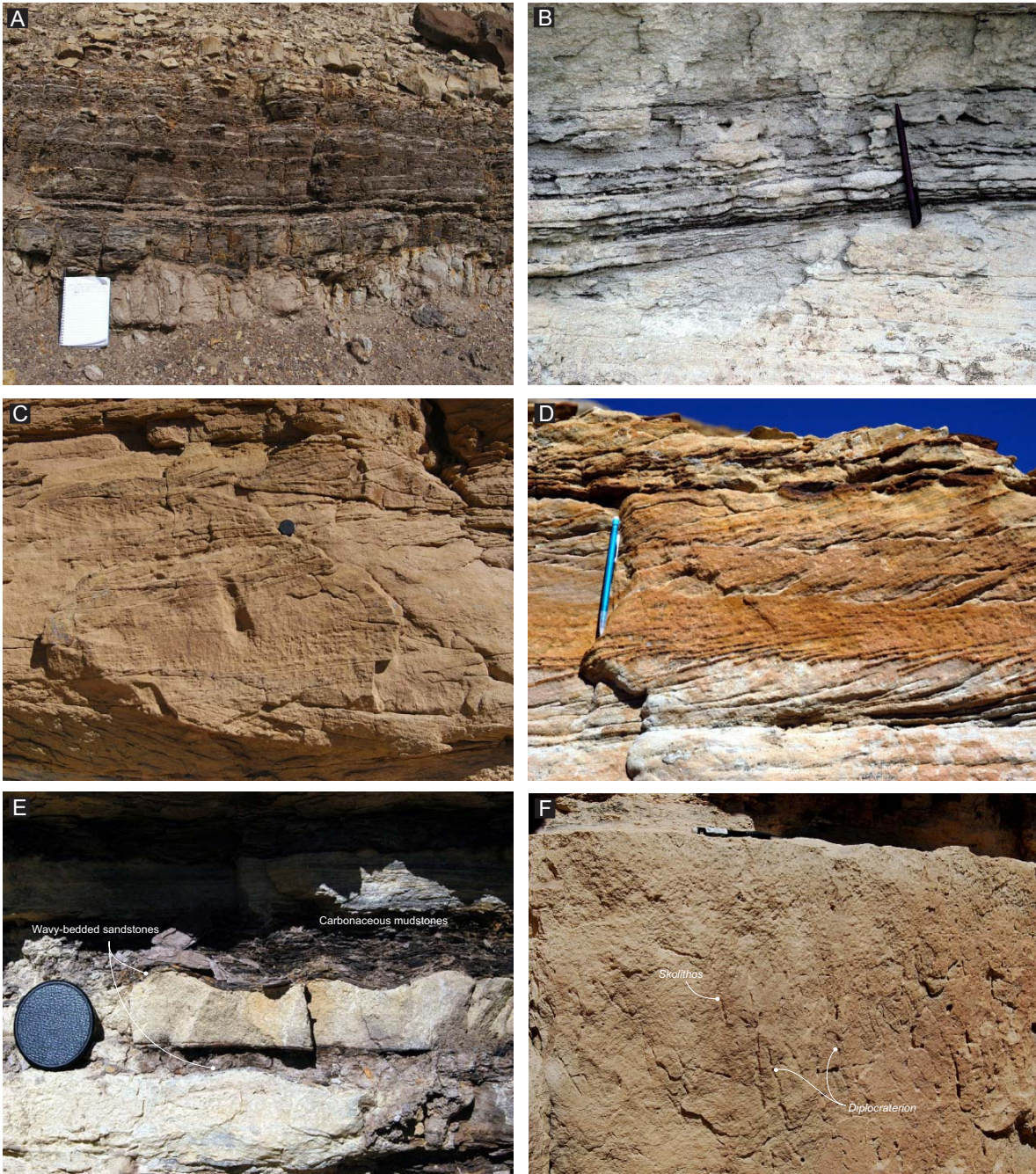


Figure 3



Figure 4

Table 1.—Summary of facies and facies associations in the Cliff House Sandstone in the Chaco Natural Historical Park study area.

Facies Association	Facies Code	Facies	Sedimentary Structures	Geometry	BI	Bioturbation
Continental Facies Association	C1	Undifferentiated Coastal-plain and lagoon	Micaceous mudstones, siltstones, and rare fine-grained sandstones. Abundant carbonaceous plant material.	Extensive sheets. 0.75 m to over 10 m thick, < 10 km dip and strike extent	0	<i>Absent</i>
Tide-Dominated Facies Association	T1	Tidal channel fill	Poor to moderately well sorted, fine- to lower coarse-grained sandstone. Bidirectional trough and planar cross-bedding, with occasional silty-clay drapes. Current ripple-cross-lamination and mud rip-up clasts.	Sandstone lenses. 1–20 m thick. > 10 km strike extent. 3–6 km dip extent	3	<i>Skolithos, Thalassinoides, Ophiomorpha, Tereidolites</i>
	T2	Tide-influenced channel fill	Poor to moderately sorted, fine- to medium-grained sandstone. Abundant cross-bedding with carbonaceous drapes and current-ripple cross-laminations with water escape structures and rip-up clasts.	Sandstone ribbons 1–20 m thick. 1–4 km dip extent Individual channel belts restricted to > 10 km.	1	<i>Thalassinoides</i>
	T3	Tidal flats	Intercalated, fine- to medium-grained sandstones, siltstones, and mudstones. Wave and current cross-ripple lamination, with abundant carbonaceous material. Flaser and lenticular bedding throughout.	Minor sheets. Rarely exceed 2 m in thickness. 100–200 m dip and strike extent.	2	<i>Thalassinoides</i>
Wave-Dominated Facies Association	W1	Foreshore	Moderately sorted, upper fine- to medium-grained sandstone. Planar, parallel to low-angle laminated (< 3°).	Tabular. 1–2 m in thickness. 1–2 km in dip extent. Preservation dependant on overlying erosion surfaces.	3	<i>Skolithos, Diplocraterion</i>
	W2	Upper shoreface	Moderately sorted, upper fine- to medium-grained sandstone. Small trough and planar cross-bedded sets and cosets.	Tabular. 1–2 m in thickness. 1–2 km in dip extent. Gradational facies with proximal lower-shoreface facies.	3	<i>Skolithos, Diplocraterion</i>
	W3	Proximal lower shoreface	Amalgamated units of well sorted, fine-grained sandstone. Swaly- and hummocky cross-stratification, rare wavy lamination sand planar to low-angle lamination.	Extensive tabular sheets. 1–20 m thick. < 10 km dip extent and 10's of km along strike.	3–4	<i>Thalassinoides, Arenicolites, Palaeophycos, Ophiomorpha, Planolites</i>
	W4	Distal lower shoreface	Non-amalgamated units of well sorted, fine grained sandstone interbedded with siltstone- and mudstone units. Hummocky cross-stratification with rare wave-ripple lamination.	Low-angle tabular wedge. 1–5 m thick. < 5 km dip extent and 10's of km along strike	3	<i>Thalassinoides, Ophiomorpha, Planolites</i>
	W5	Offshore shales	Interbedded siltstone- and mudstones with rare sub-metre fine sandstone beds. Planar, parallel laminations with occasional wavy and ripple cross lamination.	Low angle tabular wedge. 1–5 m thick. < 5 km dip extent and 10's of km along strike	2	<i>Planolites</i>
	D1	Mouth-bars	Interbedded upper fine sandstones, silt- and mudstones. Hummocky and swaly cross-stratification, wave and current ripple cross-lamination, planar parallel and low-angle inclined lamination. Mud rip-up clasts common.	Discontinuous channel bodies. 1–4 m thick. Facies preserved in front of tidal ravinement surfaces and behind wave ravinement surfaces.	3	<i>Thalassinoides, Arenicolites, Palaeophycos, Ophiomorpha, Planolites</i>

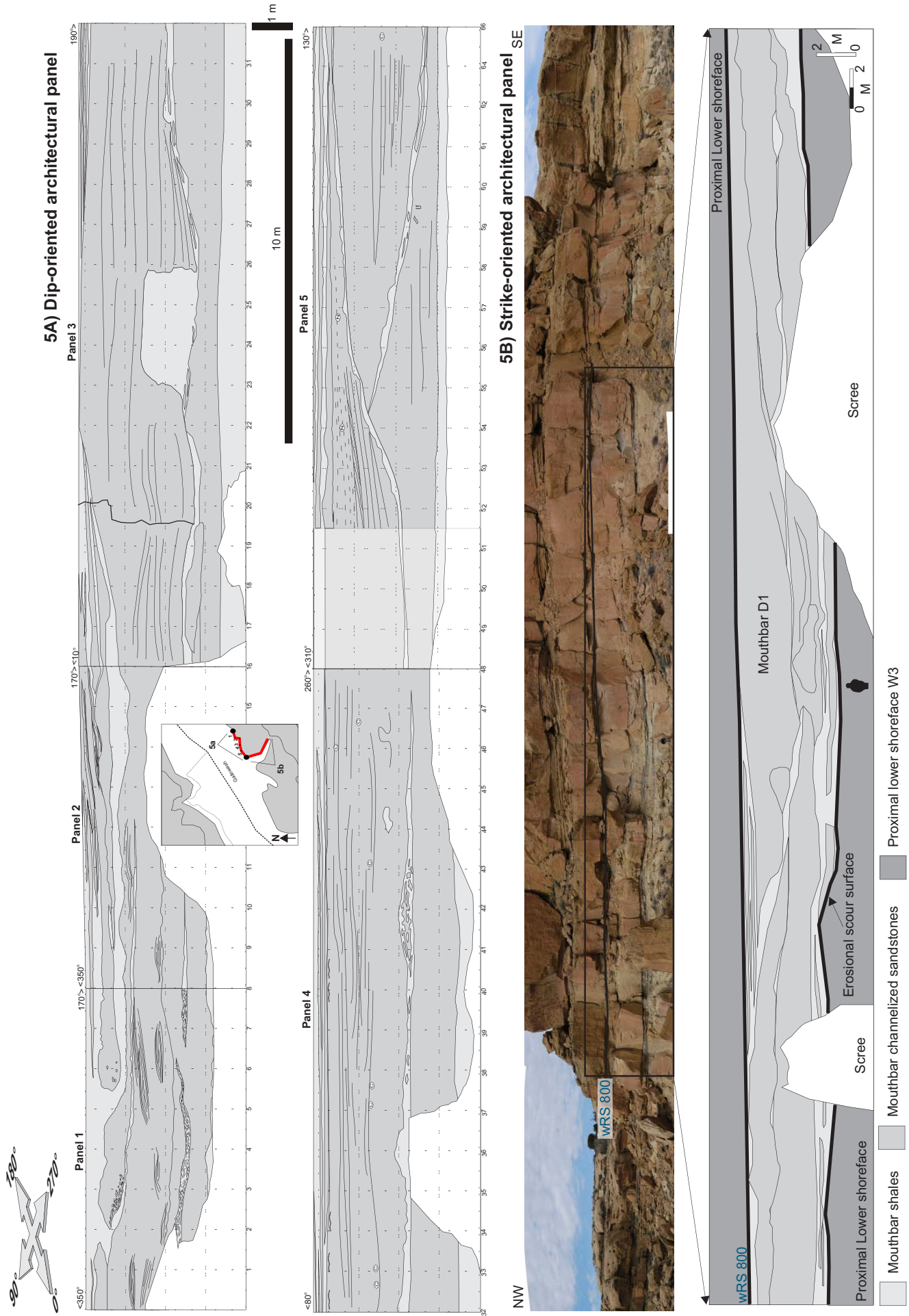


Figure 5

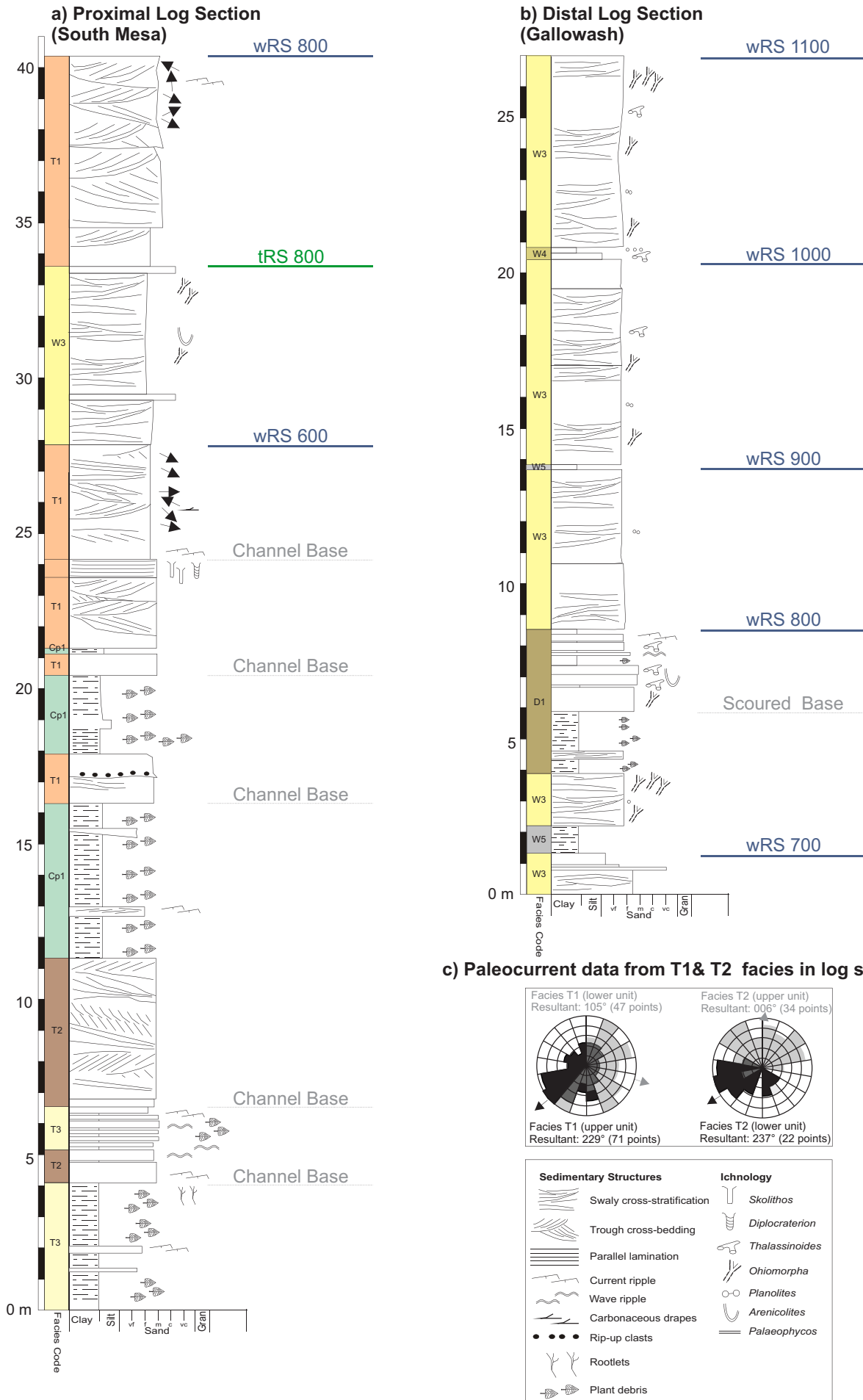


Figure 6

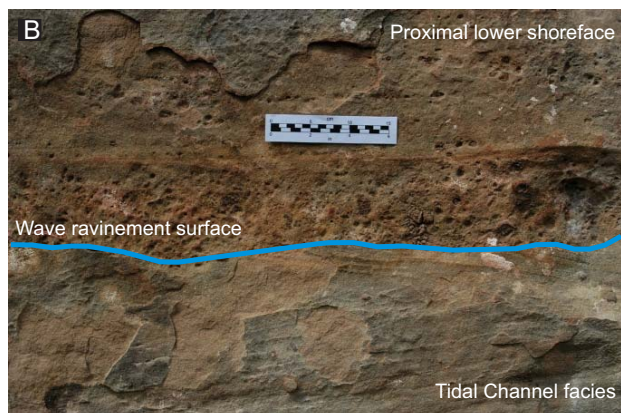
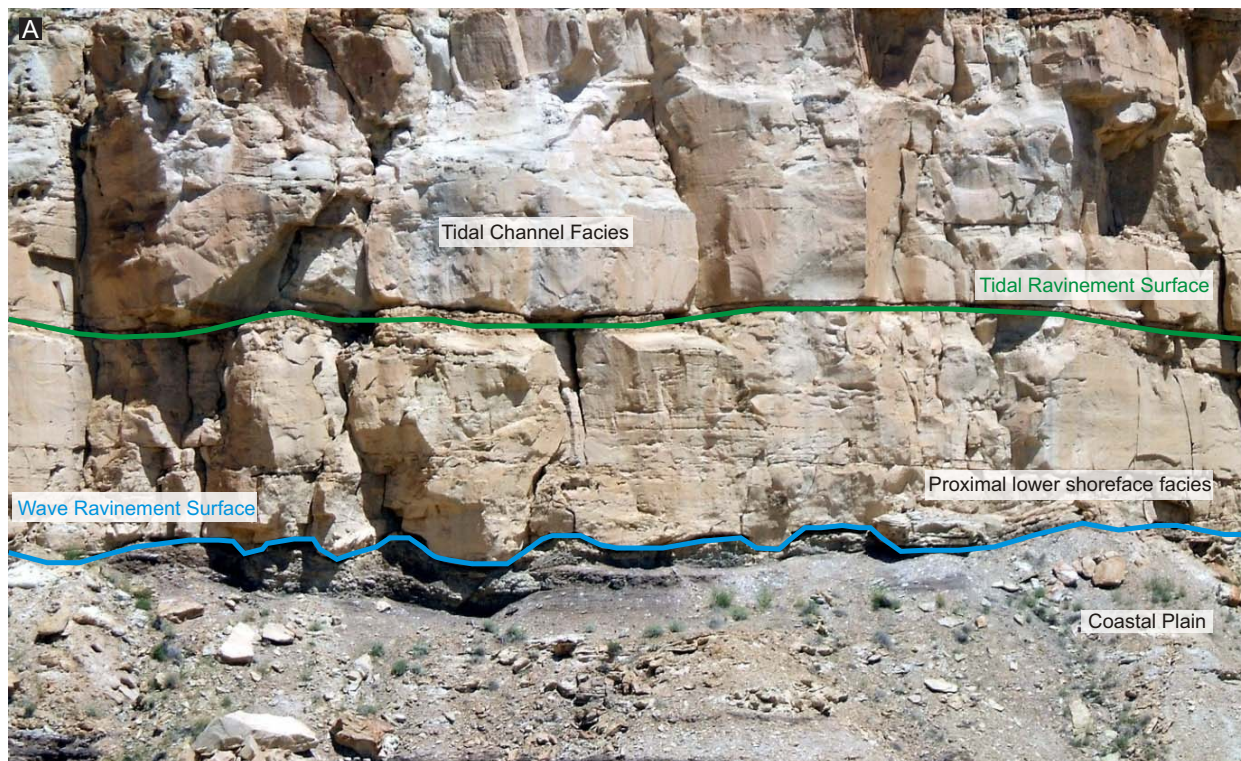


Figure 7

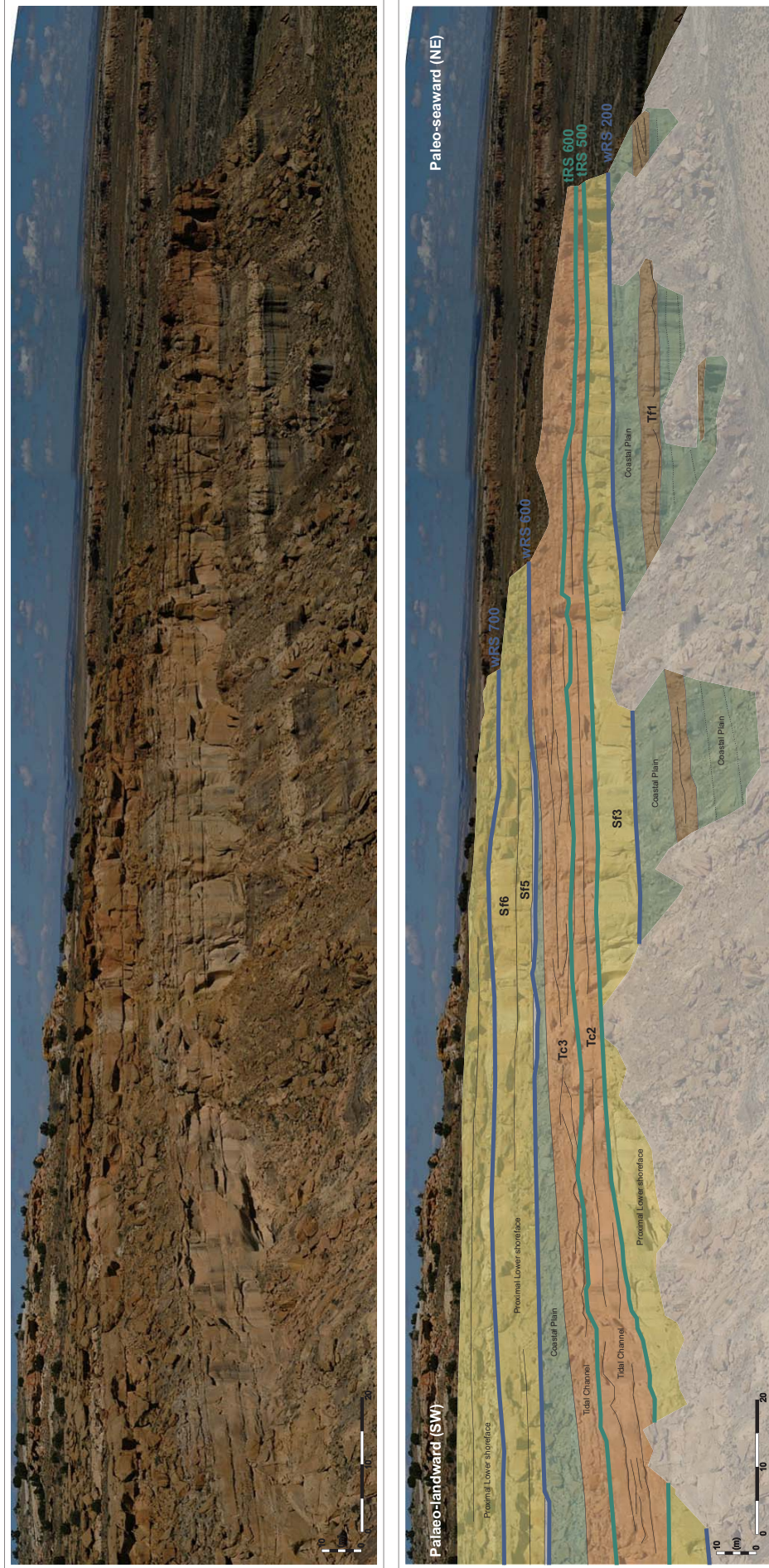


Figure 8

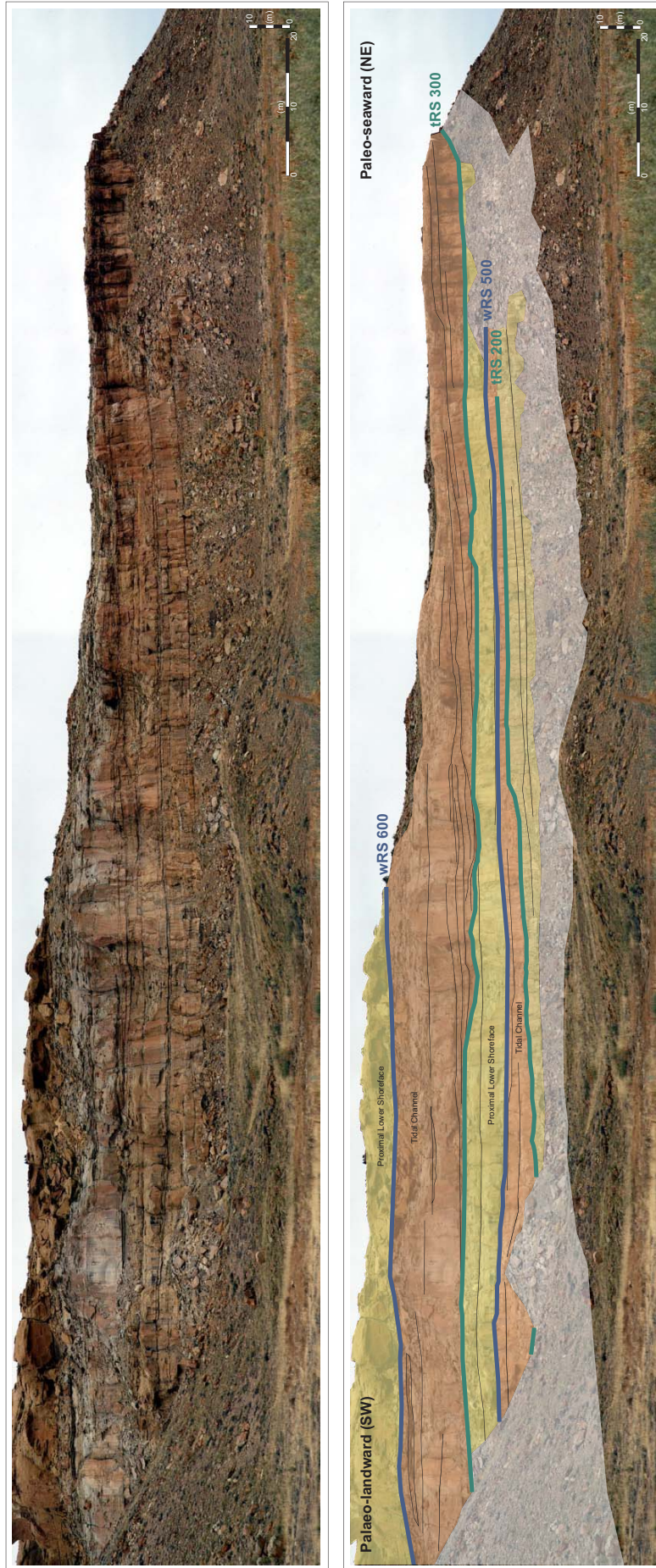
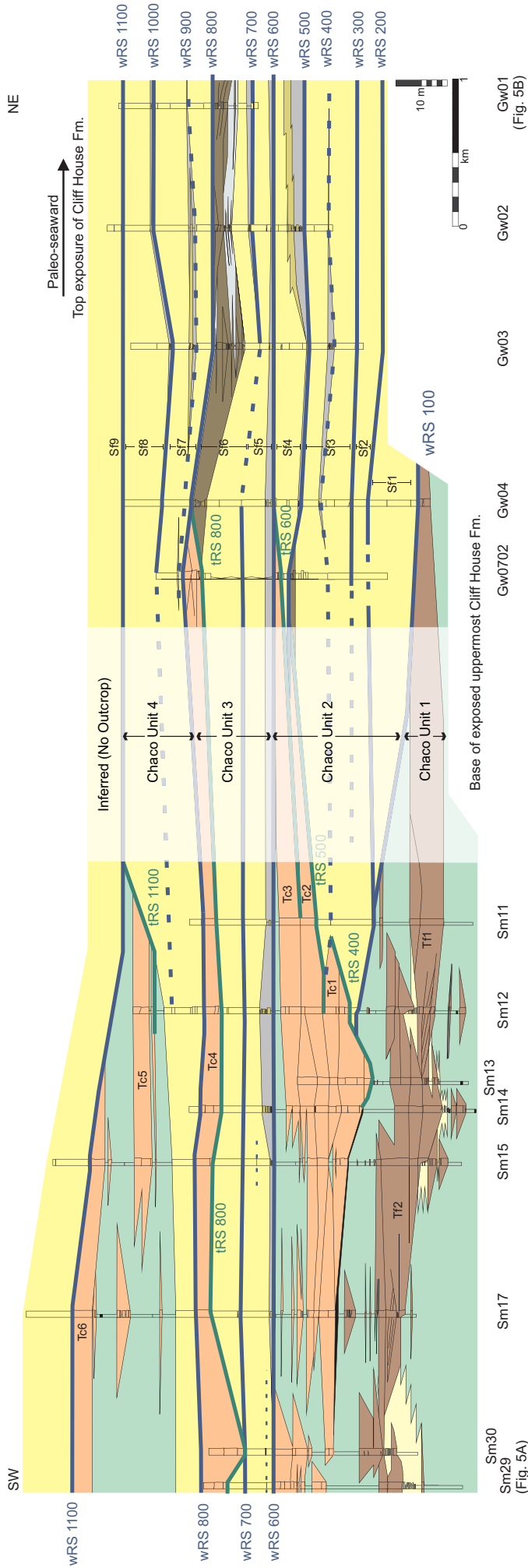
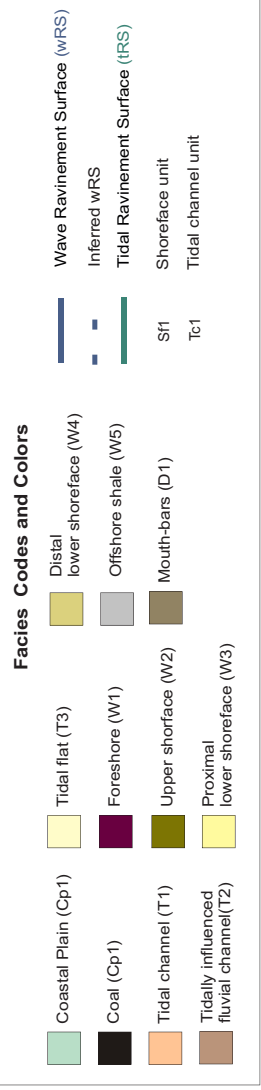


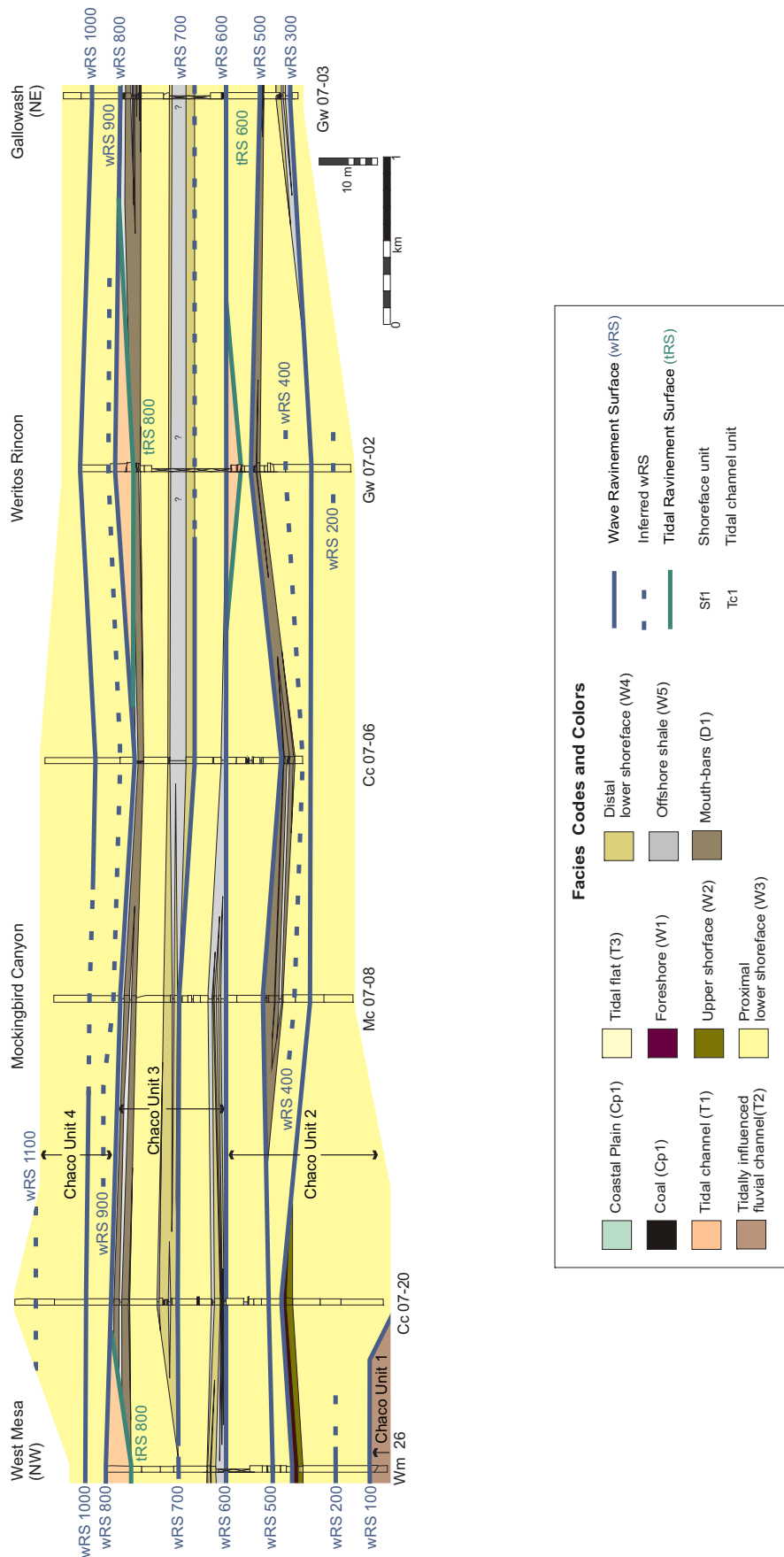
Figure 9



Sm30
Sm29
Sm17
Sm15
Sm14
Sm13
Sm12
Sm11
Gw0702
Gw04
Gw03
Gw02
Gw01
(Fig. 5A)



(Fig. 5B)



Facies Codes and Colors

Coastal Plain (Cp1)	Tidal flat (T3)	Wave Ravinement Surface (wRS)
Coal (Cp1)	Foreshore (W1)	Inferred wRS
Tidal channel (T1)	Upper shoreface (W2)	Tidal Ravinement Surface (iRS)
Tidally influenced fluvial channel(T2)	Proximal lower shoreface (W3)	Shoreface unit
	Distal lower shoreface (W4)	Tidal channel unit
	Offshore shale (W5)	
	Mouth-bars (D1)	
	Sf1	
	Tc1	

Figure 11

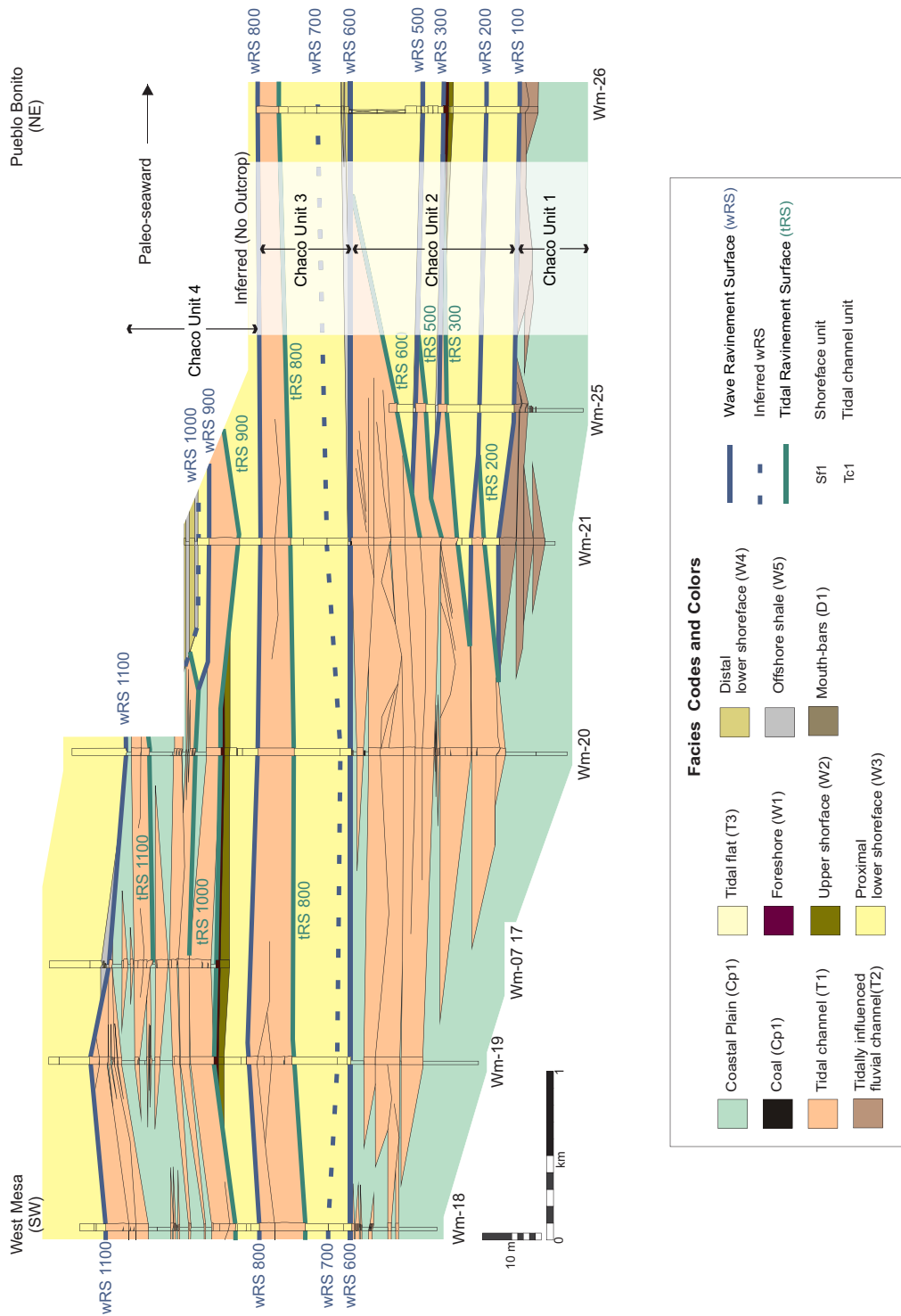
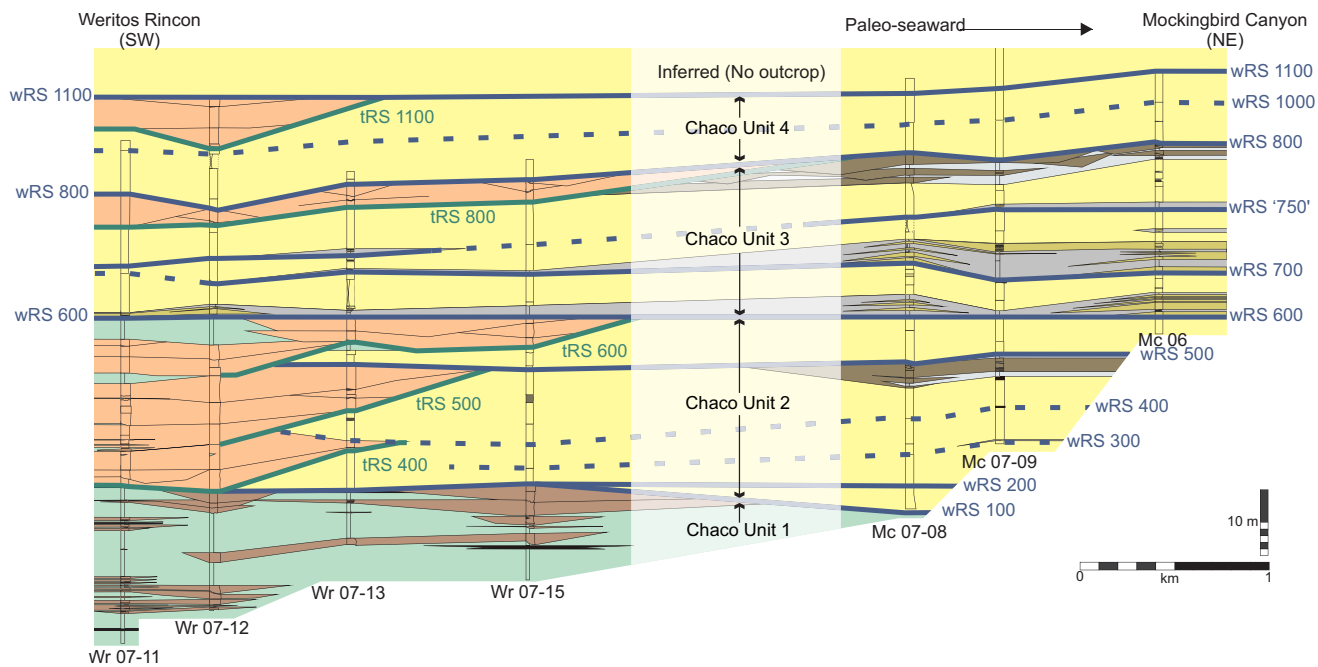


Figure 12



Facies Codes and Colors


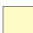












 Coastal Plain (Cp1)	 Tidal flat (T3)	 Distal lower shoreface (W4)	 Wave Ravinement Surface (wRS)
 Coal (Cp1)	 Foreshore (W1)	 Offshore shale (W5)	 Inferred wRS
 Tidal channel (T1)	 Upper shoreface (W2)	 Mouth-bars (D1)	 Tidal Ravinement Surface (tRS)
 Tidally influenced fluvial channel (T2)	 Proximal lower shoreface (W3)		Sf1 Shoreface unit
			Tc1 Tidal channel unit

Figure 13

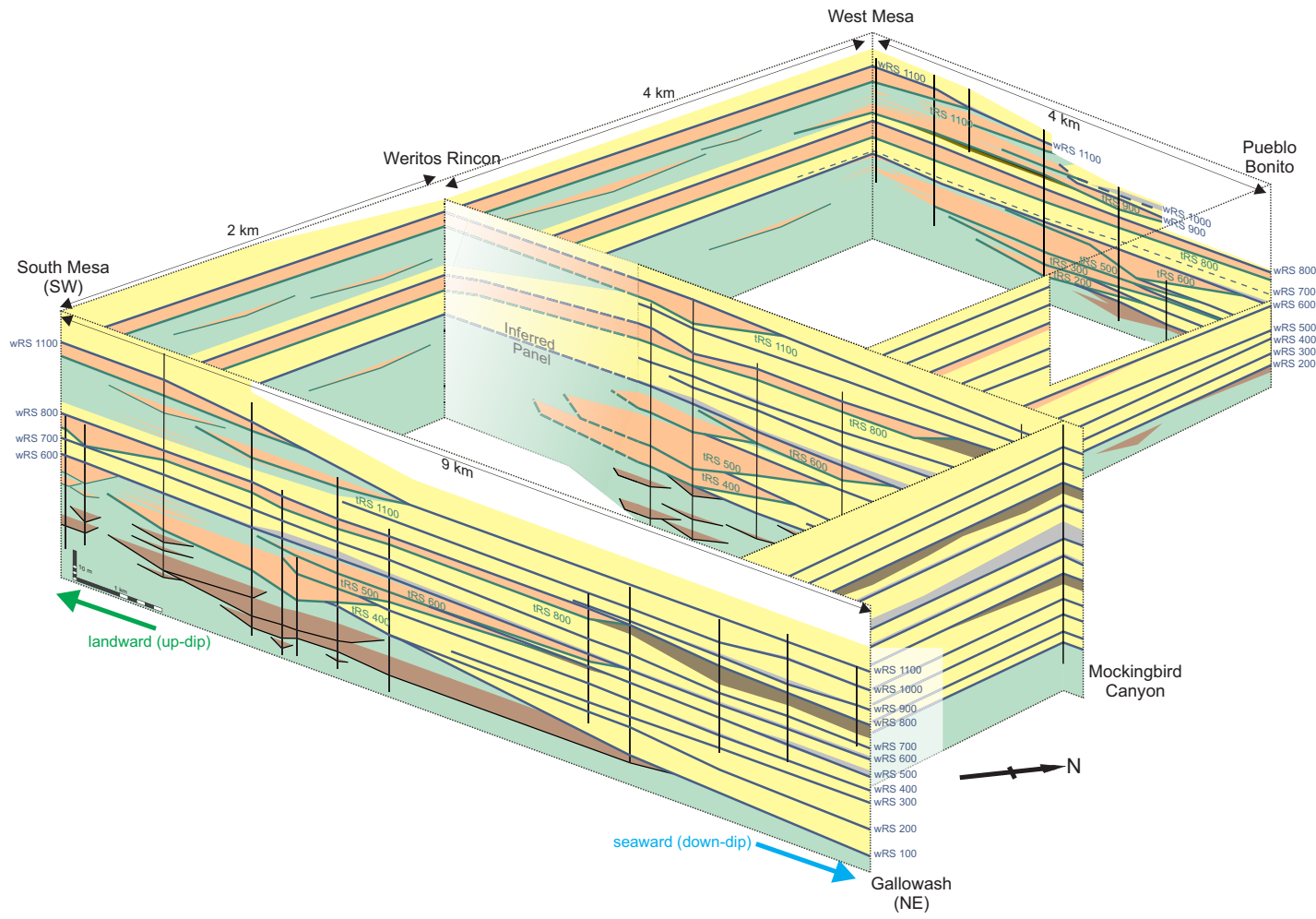


Figure 14

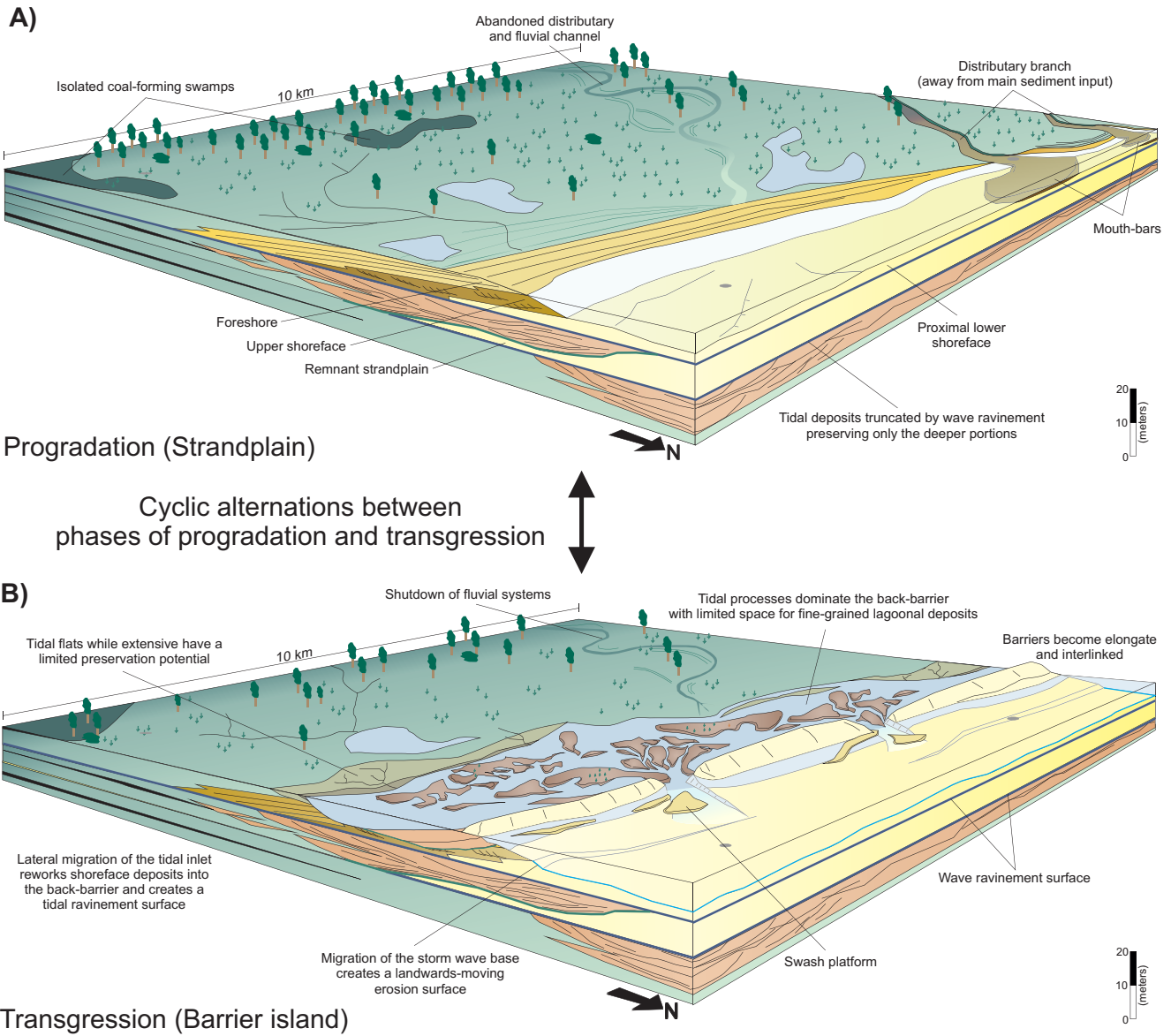


Figure 15

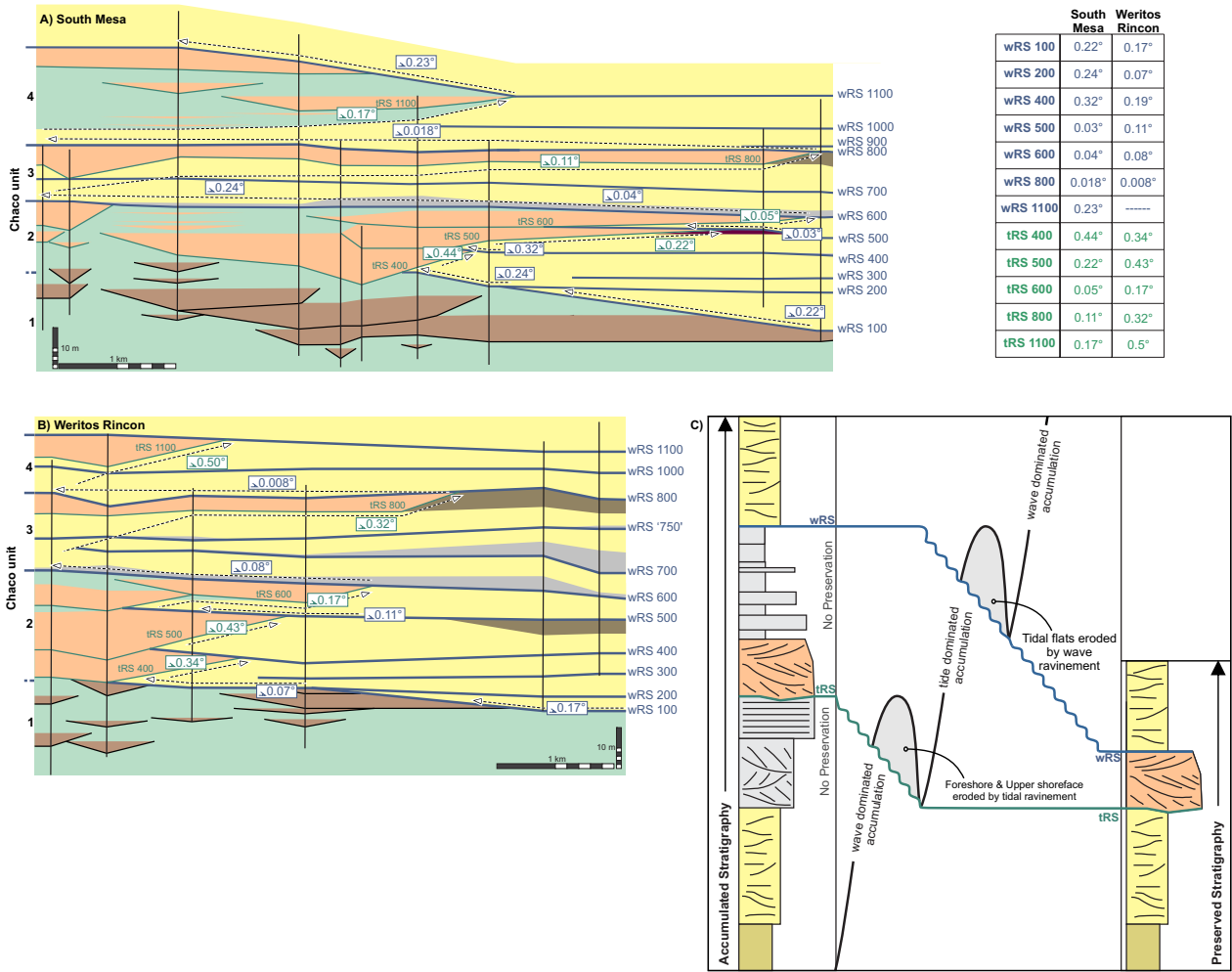


Figure 16